

# Chapter 2

## Reinforcements

### 2.1 Introduction

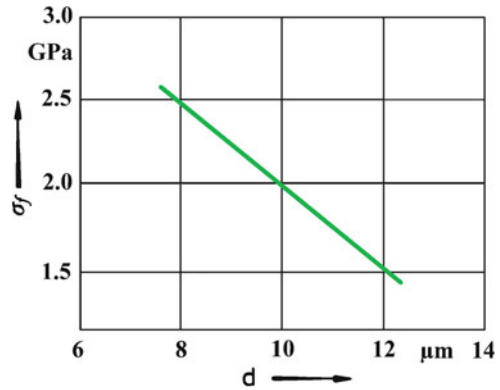
Reinforcements need not necessarily be in the form of long fibers. One can have them in the form of particles, flakes, whiskers, short fibers, continuous fibers, or sheets. It turns out that most reinforcements used in composites have a fibrous form because materials are stronger and stiffer in the fibrous form than in any other form. Specifically, in this category, we are most interested in the so-called advanced fibers, which possess very high strength and very high stiffness coupled with a very low density. The reader should realize that many naturally occurring fibers can be and are used in situations involving not very high stresses (Chawla 1976; Chawla and Bastos 1979). The great advantage in this case, of course, is its low cost. The vegetable kingdom is, in fact, the largest source of fibrous materials. Cellulosic fibers in the form of cotton, flax, jute, hemp, sisal, and ramie, for example, have been used in the textile industry, while wood and straw have been used in the paper industry. Other natural fibers, such as hair, wool, and silk, consist of different forms of protein. Silk fibers produced by a variety of spiders, in particular, appear to be very attractive because of their high work of fracture. Any discussion of such fibers is beyond the scope of this book. The interested reader is directed to some books that cover the vast field of fibers used as reinforcements (Chawla 1998; Warner 1995). In this chapter, we confine ourselves to a variety of man-made reinforcements. Glass fiber, in its various forms, has been the most common reinforcement for polymer matrices. Aramid fiber, launched in the 1960s, is much stiffer and lighter than glass fiber. Kevlar is Du Pont's trade name for aramid fiber while Twaron is the trade name of aramid fiber made by Teijin Aramid. Gel-spun polyethylene fiber, which has a stiffness comparable to that of aramid fiber, was commercialized in the 1980s. Other high-performance fibers that combine high strength with high stiffness are boron, silicon carbide, carbon, and alumina. These were all developed in the second part of the twentieth century. In particular, some ceramic fibers were developed in the last quarter of the twentieth century by

some very novel processing techniques, namely, sol-gel processing and controlled pyrolysis of organic precursors.

The use of fibers as high-performance engineering materials is based on three important characteristics (Dresher 1969):

1. A small diameter with respect to its grain size or other microstructural unit. This allows a higher fraction of the theoretical strength to be attained than is possible in a bulk form. This is a direct result of the so-called size effect; the smaller the size, the lower the probability of having imperfections in the material. Figure 2.1 shows that the strength of a carbon fiber decreases as its diameter increases (de Lamotte and Perry 1970). Although this figure shows a linear drop in strength with increasing fiber diameter, a nonlinear relationship is not uncommon. Figure 2.1 should be taken only as a general trend indicator.

**Fig. 2.1** Decrease in strength ( $\sigma_f$ ) of a carbon fiber with increase in diameter [from de Lamotte and Perry (1970), used with permission]



2. A high aspect ratio (length/diameter,  $l/d$ ), which allows a very large fraction of the applied load to be transferred via the matrix to the stiff and strong fiber (see Chap. 10).
3. A very high degree of flexibility, which is really a characteristic of a material that has a low modulus or stiffness and a small diameter. This flexibility permits the use of a variety of techniques for making composites with these fibers.

Next we consider the concept of flexibility, and then we describe the general fiber spinning processes.

### 2.1.1 Flexibility

Flexibility of a given material, as pointed out in the attributes above, is a function of its elastic stiffness and dimensions of the cross-section. Intuitively, one can easily visualize that the higher the stiffness of material, the less flexible it will be. But when we think of flexibility of a fiber or thread, we wish to know to what arbitrary

radius we can bend it before it fails. We can treat our single fiber to be an elongated elastic beam. Let us subject this fiber of Young's modulus,  $E$  and diameter,  $d$  to a bending moment,  $M$ , which will bend it to a radius,  $R$ . For such an elastic bending of a beam, we define *flexural rigidity* as  $MR$ . From elementary strength of materials, we have the following relationship for a beam bent to a radius  $R$ :

$$\frac{M}{I} = \frac{E}{R} ,$$

or,

$$MR = EI ,$$

where  $E$  is the Young's modulus of the material and  $I$  is the second moment of area or moment of inertia of its cross-section. For a beam or a fiber of diameter,  $d$ , the second moment of area about an axis through the centroid of the beam is given by  $I = \pi d^4/64$ . Now, we can define flexibility of the fiber (i.e., the elastic beam under consideration) as the inverse of flexural rigidity. In other words, flexibility of a fiber is an inverse function of its elastic modulus,  $E$ , and the second moment of area or moment of inertia of its cross-section,  $I$ . The elastic modulus of a material is generally independent of its form or size and is generally a material constant for a given chemical composition (assuming a fully dense material). Thus, for a given composition and density, the flexibility of a material is determined by its shape, or more precisely by its diameter. Substituting for  $I = \pi d^4/64$  in the above expression, we get,

$$MR = EI = \frac{E\pi d^4}{64} ,$$

or, the flexibility, being equal to  $1/MR$ , is

$$\text{Flexibility} = \frac{1}{MR} = \frac{64}{E\pi d^4} , \quad (2.1)$$

where  $d$  is the equivalent diameter and  $I$  is the moment of inertia of the beam (fiber). Equation (2.1) indicates that flexibility,  $1/MR$ , is a very sensitive function of diameter,  $d$ . We can summarize the important implications of Eq. (2.1) as follows:

- Flexibility of a fiber is a very sensitive inverse function of its diameter,  $d$ .
- Given a sufficiently small diameter, it is possible to produce, in principle, a fiber as flexible as any from a polymer, a metal, or a ceramic.
- One can make very flexible fibers out of inherently brittle materials such as glass, silicon carbide, alumina, etc., provided one can shape these brittle materials into a fine diameter fiber. Producing a fine diameter ceramic fiber, however, is a daunting problem in processing.

To illustrate this concept of flexibility, we plot the diameter of various materials in fibrous form with flexibility ( $1/MR$ ) equal to that of highly flexible filament, namely, a 25- $\mu\text{m}$ -diameter nylon fiber as function of the elastic modulus,  $E$ . Note that given a sufficiently small diameter, it is possible for a metal or ceramic to have the same degree of flexibility as that of a 25- $\mu\text{m}$ -diameter nylon fiber; it is, however, another matter that obtaining such a small diameter in practice can be prohibitively expensive.

### 2.1.2 Fiber Spinning Processes

Fiber spinning is the process of extruding a liquid through small holes in a spinneret to form solid filaments. In nature, silkworms and spiders produce continuous filaments by this process. There exists a variety of different fiber spinning techniques; some of the important ones are:

*Wet spinning.* A solution is extruded into a coagulating bath. The jets of liquid freeze or harden in the coagulating bath as a result of chemical or physical changes.

*Dry spinning.* A solution consisting of a fiber-forming material and a solvent is extruded through a spinneret. A stream of hot air impinges on the jets of solution emerging from the spinneret, the solvent evaporates, and solid filaments are left behind.

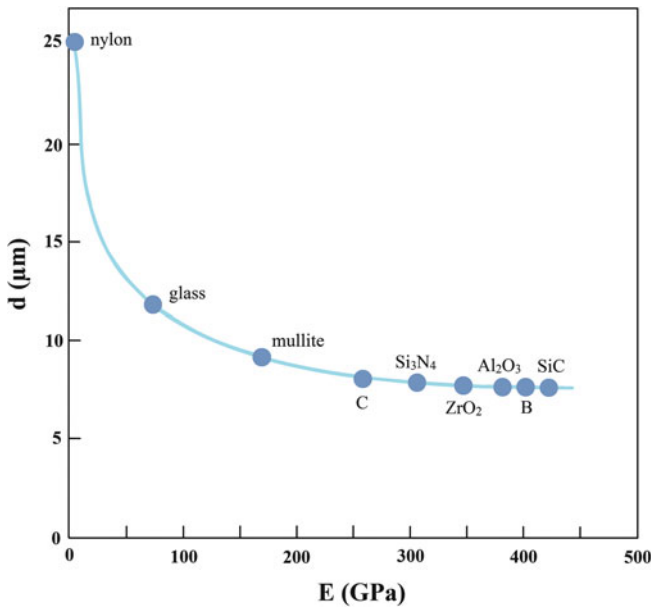


**Fig. 2.2** Fiber diameter of different materials with flexibility equal to that of a nylon fiber of diameter equal to 25  $\mu\text{m}$ . Note that one can make very flexible fibers out of brittle materials such as glass, silicon carbide, alumina, etc., provided one can process them into a small diameter

*Melt spinning.* The fiber-forming material is heated above its melting point and the molten material is extruded through a spinneret. The liquid jets harden into solid filaments in air on emerging from the spinneret holes.

*Dry jet–wet spinning.* This is a special process devised for spinning of aramid fibers. In this process, an appropriate polymer liquid crystal solution is extruded through spinneret holes, passes through an air gap before entering a coagulation bath, and then goes on a spool for winding. We describe this process in detail in Sect. 2.5.2.

### 2.1.3 Stretching and Orientation

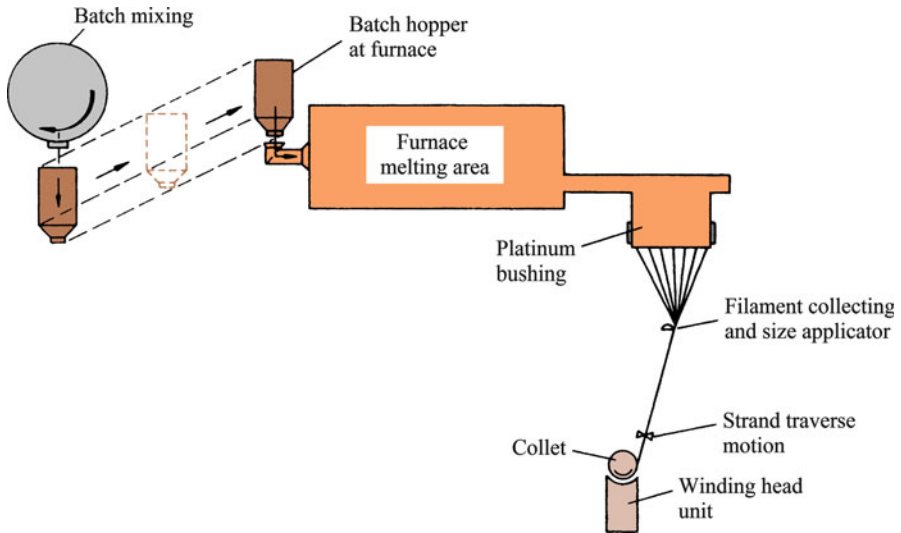
The process of extrusion through a spinneret results in some chain orientation in the filament. Generally, the molecules in the surface region undergo more orientation than the ones in the interior because the edges of the spinneret hole affect the near-surface molecules more. This is known as the *skin effect*, and it can affect many other properties of the fiber, such as the adhesion with a polymeric matrix or the ability to be dyed. Generally, the as-spun fiber is subjected to some stretching, causing further chain orientation along the fiber axis and consequently better tensile properties, such as stiffness and strength, along the fiber axis. The amount of stretch is generally given in terms of a draw ratio, which is the ratio of the initial diameter to the final diameter. For example, nylon fibers are typically subjected to a draw ratio of 5 after spinning. A high draw ratio results in a high elastic modulus. Increased alignment of chains means a higher degree of crystallinity in a fiber. This also affects the ability of a fiber to absorb moisture. The higher the degree of crystallinity, the lower the moisture absorption. In general, the higher degree of crystallinity translates into a higher resistance to penetration by foreign molecules, i.e., a greater chemical stability. The stretching treatment serves to orient the molecular structure along the fiber axis. It does not, generally, result in complete elimination of molecular branching; that is, one gets molecular orientation but not extension. Such stretching treatments do result in somewhat more efficient packing than in the unstretched polymer, but there is a limit to the amount of stretch that can be given to a polymer because the phenomenon of necking can intervene and cause rupture of the fiber.

## 2.2 Glass Fibers

Glass fiber is a generic name like carbon fiber or steel or aluminum. Just as different compositions of steel or aluminum alloys are available, there are many of different chemical compositions of glass fibers that are commercially available. Common glass fibers are silica based (~50–60 % SiO<sub>2</sub>) and contain a host of other oxides of calcium, boron, sodium, aluminum, and iron, for example. Table 2.1 gives the compositions of some commonly used glass fibers. The designation *E* stands for

**Table 2.1** Approximate chemical compositions of some glass fibers (wt.%)

Composition	E glass	C glass	S glass
SiO <sub>2</sub>	55.2	65.0	65.0
Al <sub>2</sub> O <sub>3</sub>	8.0	4.0	25.0
CaO	18.7	14.0	–
MgO	4.6	3.0	10.0
Na <sub>2</sub> O	0.3	8.5	0.3
K <sub>2</sub> O	0.2	–	–
B <sub>2</sub> O <sub>3</sub>	7.3	5.0	–

**Fig. 2.3** Schematic of glass fiber manufacture

electrical because *E* glass is a good electrical insulator in addition to having good strength and a reasonable Young's modulus; *C* stands for corrosion and *C* glass has a better resistance to chemical corrosion than other glasses; *S* stands for the high silica content that makes *S* glass withstand higher temperatures than other glasses. It should be pointed out that most of the continuous glass fiber produced is of the *E* glass type but, notwithstanding the designation *E*, electrical uses of *E* glass fiber are only a small fraction of the total market.

### 2.2.1 Fabrication

Figure 2.3 shows schematically the conventional fabrication procedure for glass fibers (specifically, the *E* glass fibers that constitute the workhorse of the resin reinforcement industry) (Loewenstein 1983; Parkyn 1970; Lowrie 1967). The raw materials are melted in a hopper and the molten glass is fed into the electrically

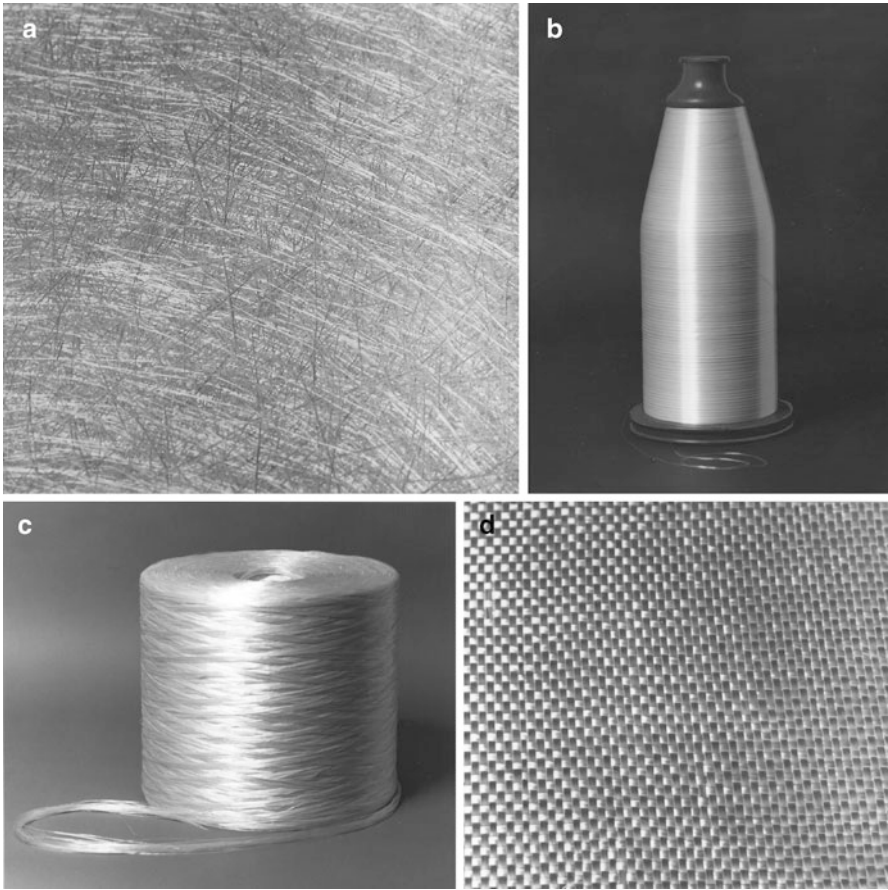


**Fig. 2.4** Glass fiber is available in a variety of forms: (a) chopped strand, (b) continuous yarn, (c) roving, (d) fabric [courtesy of Morrison Molded Fiber Glass Company]



**Fig. 2.5** Continuous glass fibers (cut from a spool) obtained by the sol-gel technique [from Sakka (1985), used with permission]

heated platinum bushings or crucibles; each bushing contains about 200 holes at its base. The molten glass flows by gravity through these holes, forming fine continuous filaments; these are gathered together into a strand and a *size* is applied before it is a wound on a drum. The final fiber diameter is a function of the bushing orifice diameter; viscosity, which is a function of composition and temperature; and the head of glass in the hopper. In many old industrial plants the glass fibers are not produced directly from fresh molten glass. Instead, molten glass is first turned into marbles, which after inspection are melted in the bushings. Modern plants do produce glass fibers by direct drawing. Figure 2.4 shows some forms in which glass fiber is commercially available.

The conventional methods of making glass or ceramic fibers involve drawing from high-temperature melts of appropriate compositions. This route has many practical difficulties such as the high processing temperature required, the immiscibility of components in the liquid state, and the easy crystallization during cooling. Several techniques have been developed for preparing glass and ceramic fibers (Chawla 1998). An important technique is called the sol-gel technique (Brinker and Scherer 1990; Jones 1989). We shall come back to this sol-gel technique at various places in this book. Here we just provide a brief description. A *sol* is a colloidal suspension in which the individual particles are so small (generally in the *nm* range) that they show no sedimentation. A *gel*, on the other hand, is a suspension in which the liquid medium has become viscous enough to behave more or less like a solid. The sol-gel process of making a fiber involves a conversion of fibrous gels, drawn from a solution at a low temperature, into glass or ceramic fibers at several hundred degrees Celsius. The maximum heating temperature in this process is much lower than that in conventional glass fiber manufacture. The sol-gel method using metal alkoxides consists of preparing an appropriate homogeneous solution, changing the solution to a sol, gelling the sol, and converting the gel to glass by heating. The sol-gel technique is a very powerful technique for making glass and ceramic fibers. The 3M Company produces a series of alumina and silica-alumina fibers, called the Nextel fibers, from metal alkoxide solutions (see Sect. 2.6). Figure 2.5 shows an example of drawn silica fibers (cut from a continuous fiber spool) obtained by the sol-gel technique (Sakka 1985).

Glass filaments are easily damaged by the introduction of surface defects. To minimize this and to make handling of these fibers easy, a sizing treatment is given. The size, or coating, protects and binds the filaments into a strand.

### 2.2.2 Structure

Inorganic, silica-based glasses are analogous to organic glassy polymers in that they are amorphous, i.e., devoid of any long-range order that is characteristic of a crystalline material. Pure, crystalline silica melts at 1,800 °C. However, by adding some metal oxides, we can break the Si-O bonds and obtain a series of amorphous



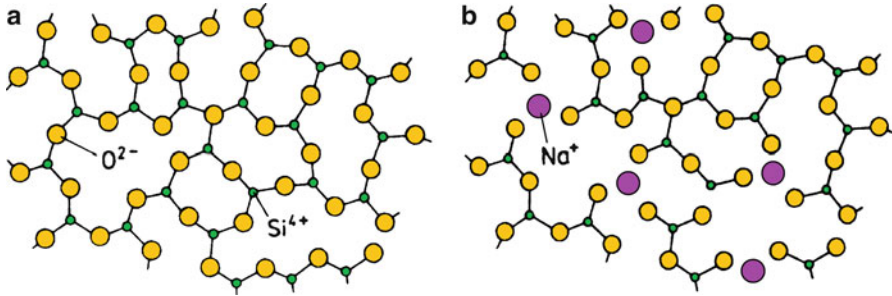


**Fig. 2.6** Amorphous structure of glass: (a) a two-dimensional representation of silica glass network and (b) a modified network that results when  $\text{Na}_2\text{O}$  is added to (a). Note that  $\text{Na}^+$  is ionically linked with  $\text{O}^{2-}$  but does not join the network directly

**Table 2.2** Typical properties of E glass fibers

Density ( $\text{g}/\text{cm}^3$ )	Tensile strength (MPa)	Young's modulus (GPa)	Coefficient of thermal expansion ( $\text{K}^{-1}$ )
2.55	1,750	70	$4.7 \times 10^{-6}$

glasses with rather low glass transition temperatures. Figure 2.6a shows a two-dimensional network of silica glass. Each polyhedron consists of oxygen atoms bonded covalently to silicon. What happens to this structure when  $\text{Na}_2\text{O}$  is added to the glass is shown in Fig. 2.6b. Sodium ions are linked ionically with oxygen but they do not join the network directly. Too much  $\text{Na}_2\text{O}$  will impair the tendency for glassy structure formation. The addition of other metal oxide types (Table 2.1) serves to alter the network structure and the bonding and, consequently, the properties. Note the isotropic, three-dimensional network structure of glass (Fig. 2.6); this leads to the more or less isotropic properties of glass fibers. That is, for the glass fiber, Young's modulus and thermal expansion coefficients are the same along the fiber axis and perpendicular to it. This is unlike many other fibers, such as aramid and carbon, which are highly anisotropic.

### 2.2.3 Properties and Applications

Typical mechanical properties of E glass fibers are summarized in Table 2.2. Note that the density is quite low and the strength is quite high; Young's modulus, however, is not very high. Thus, while the strength-to-weight ratio of glass fibers is quite high, the modulus-to-weight ratio is only moderate. It is this latter characteristic that led the aerospace industry to other so-called advanced fibers (e.g., boron, carbon,  $\text{Al}_2\text{O}_3$ , and  $\text{SiC}$ ). Glass fibers continue to be used for reinforcement of polyester, epoxy, and phenolic resins. It is quite cheap, and it is available in a variety of forms (see Fig. 2.4). Continuous strand is a group of

individual fibers; roving is a group of parallel strands; chopped fibers consists of strand or roving chopped to lengths between 5 and 50 mm. Glass fibers are also available in the form of woven fabrics or nonwoven mats.

Moisture decreases glass fiber strength. Glass fibers are also susceptible to what is called static fatigue; that is, when subjected to a constant load for an extended time period, glass fibers can undergo subcritical crack growth. This leads to failure over time at loads that might be safe when considering instantaneous loading.

Glass fiber reinforced resins are used widely in the building and construction industry. Commonly, these are called glass-reinforced plastics, or GRP. They are used in the form of a cladding for other structural materials or as an integral part of a structural or non-load-bearing wall panel; window frames, tanks, bathroom units, pipes, and ducts are common examples. Boat hulls, since the mid-1960s, have primarily been made of GRP. Use of GRP in the chemical industry (e.g., as storage tanks, pipelines, and process vessels) is fairly routine. The rail and road transportation industry and the aerospace industry are other big users of GRP.

## 2.3 Boron Fibers

Boron is an inherently brittle material. It is commercially made by chemical vapor deposition (CVD) of boron on a substrate, that is, boron fiber as produced is itself a composite fiber.

In view of the fact that rather high temperatures are required for this deposition process, the choice of substrate material that goes to form the core of the finished boron fiber is limited. Generally, a fine tungsten wire is used for this purpose. A carbon substrate can also be used. The first boron fibers were obtained by Weintraub (1911) by means of reduction of a boron halide with hydrogen on a hot wire substrate.

The real impulse in boron fiber fabrication, however, came in 1959, when Talley (Talley 1959; Talley et al. 1960) used the process of halide reduction to obtain amorphous boron fibers of high strength. Since then, interest in the use of strong but light boron fibers as a possible structural component in aerospace and other structures has been continuous, although it must be admitted that this interest has periodically waxed and waned in the face of rather stiff competition from other so-called advanced fibers, in particular, carbon fibers.

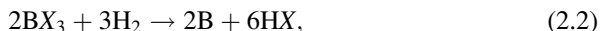
### 2.3.1 Fabrication

Boron fibers are obtained by CVD on a substrate. There are two processes:

1. *Thermal decomposition of a boron hydride.* This method involves low temperatures, and, thus, carbon-coated glass fibers can be used as a substrate.

The boron fibers produced by this method, however, are weak because of a lack of adherence between the boron and the core. These fibers are much less dense owing to the trapped gases.

2. *Reduction of boron halide.* Hydrogen gas is used to reduce boron trihalide:



where X denotes a halogen: Cl, Br, or I.

In this process of halide reduction, the temperatures involved are very high, and, thus, one needs a refractory material, for example, a high-melting-point metal such as tungsten, as a substrate. It turns out that such metals are also very heavy. This process, however, has won over the thermal reduction process despite the disadvantage of a rather high-density substrate (the density of tungsten is  $19.3 \text{ g/cm}^3$ ) mainly because this process gives boron fibers of a very high and uniform quality. Figure 2.7 shows a schematic of boron filament production by the CVD technique, and Fig. 2.8 shows a commercial boron filament production facility; each vertical reactor shown in this picture produces continuous boron monofilament.

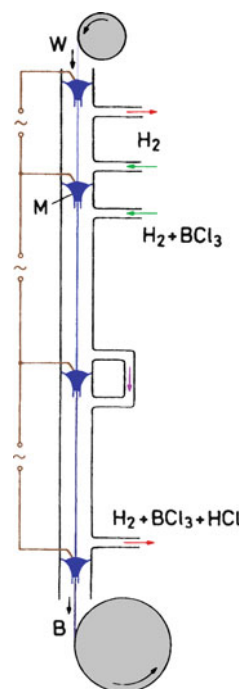
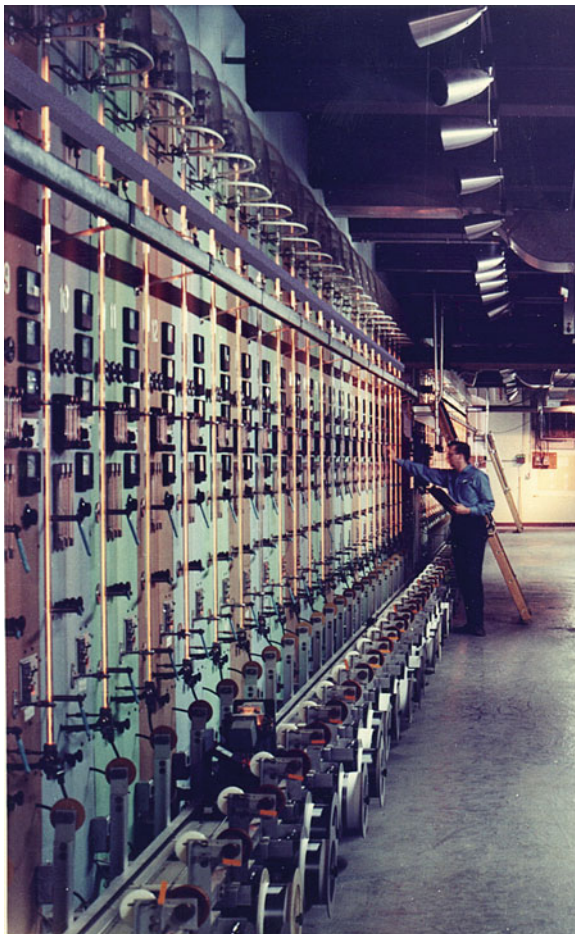


**Fig. 2.7** Schematic of boron (B) fiber production by halide decomposition on a tungsten (W) substrate [from van Maaren et al. (1975), used with permission]

**Fig. 2.8** A boron filament production facility (courtesy of AVCO Specialty Materials Co.)



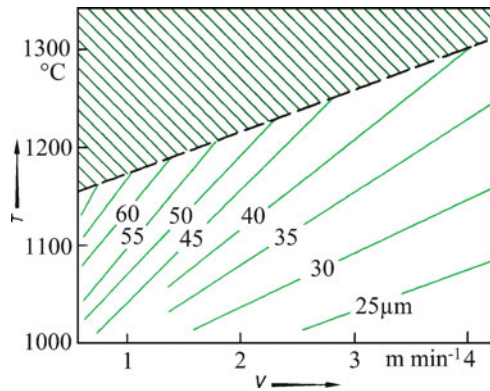
In the process of  $\text{BCl}_3$  reduction, a very fine tungsten wire (10–12  $\mu\text{m}$  diameter) is pulled into a reaction chamber at one end through a mercury seal and out at the other end through another mercury seal. The mercury seals act as electrical contacts for resistance heating of the substrate wire when gases ( $\text{BCl}_3 + \text{H}_2$ ) pass through the reaction chamber, where they react on the incandescent wire substrate. The reactor can be a one- or multistage, vertical or horizontal, reactor.  $\text{BCl}_3$  is an expensive chemical, and only about 10 % of it is converted into boron in this reaction. Thus, an efficient recovery of the unused  $\text{BCl}_3$  can result in a considerable lowering of the boron filament cost.

There is a critical temperature for obtaining a boron fiber with optimum properties and structure (van Maaren et al. 1975). The desirable amorphous form of boron occurs below this critical temperature while above this temperature crystalline forms of boron also occur that are undesirable from a mechanical properties viewpoint, as we shall see in Sect. 2.3.2. With the substrate wire

stationary in the reactor, this critical temperature is about 1,000 °C. In a system where the wire is moving, this critical temperature is higher, and it increases with the speed of the wire. One generally has a diagram of the type shown in Fig. 2.9, which shows the various combinations of wire temperature and wire drawing speed to produce a certain diameter of boron fiber. Fibers formed in the region above the dashed line are relatively weak because they contain undesirable forms of boron as a result of recrystallization. The explanation for this relationship between critical temperature and wire speed is that boron is deposited in an amorphous state and the more rapidly the wire is drawn out from the reactor, the higher the allowed temperature is. Of course, higher wire drawing speed also results in an increase in production rate and lower costs.

Boron deposition on a carbon monofilament (~35- $\mu\text{m}$  diameter) substrate involves precoating the carbon substrate with a layer of pyrolytic graphite. This coating accommodates the growth strains that result during boron deposition (Krukonis 1977). The reactor assembly is slightly different from that for boron on tungsten substrate, because pyrolytic graphite is applied online.

**Fig. 2.9** Temperature ( $T$ ) vs. wire speed ( $V$ ) for a series of boron filament diameters. Filaments formed in the gray region (above the dashed line) contain crystalline regions and are undesirable [from van Maaren et al. (1975), used with permission]



### 2.3.2 Structure and Morphology

The structure and morphology of boron fibers depend on the conditions of deposition: temperature, composition of gases, gas dynamics, and so on. While theoretically the mechanical properties are limited only by the strength of the atomic bond, in practice, there are always structural defects and morphological irregularities present that lower the mechanical properties. Temperature gradients and trace concentrations of impurity elements inevitably cause process irregularities. Even greater irregularities are caused by fluctuations in electric power, instability in gas flow, and any other operator-induced variables.

### 2.3.2.1 Structure

Depending on the conditions of deposition, the elemental boron can exist in various crystalline polymorphs. The form produced by crystallization from the melt or CVD above 1,300 °C is  $\beta$ -rhombohedral. At temperatures lower than this, if crystalline boron is produced, the most commonly observed structure is  $\alpha$ -rhombohedral.

Boron fibers produced by the CVD method described earlier have a microcrystalline structure that is generally called *amorphous*. This designation is based on the characteristic X-ray diffraction pattern produced by the filament in the Debye-Scherrer method, that is, large and diffuse halos with  $d$  spacings of 0.44, 0.25, 0.17, 1.4, 1.1, and 0.091 nm, typical of amorphous material (Vega-Boggio and Vingsbo 1978). Electron diffraction studies, however, lead one to conclude that this “amorphous” boron is really a nanocrystalline phase with a grain diameter of the order of 2 nm (Krukoniš 1977).

Based on X-ray and electron diffraction studies, one can conclude that amorphous boron is really nanocrystalline  $\beta$ -rhombohedral. In practice, the presence of microcrystalline phases (crystals or groups of crystals observable in the electron microscope) constitutes an imperfection in the fiber that should be avoided. Larger and more serious imperfections generally result from surpassing the critical temperature of deposition (see Sect. 2.3.1) or the presence of impurities in the gases.

When boron fiber is made by deposition on a tungsten substrate, as is generally the case, then depending on the temperature conditions during deposition, the core may consist of, in addition to tungsten, a series of compounds, such as  $W_2B$ ,  $WB$ ,  $W_2B_5$ , and  $WB_4$  (Galasso et al. 1967). A boron fiber cross-section (100  $\mu\text{m}$  diameter) is shown in Fig. 2.10a, while Fig. 2.10b shows schematically the various subparts of the cross-section. The various tungsten boride phases are formed by diffusion of boron into tungsten. Generally, the fiber core consists only of  $WB_4$  and  $W_2B_5$ . On prolonged heating, the core may be completely converted into  $WB_4$ . As boron diffuses into the tungsten substrate to form borides, the core expands from its

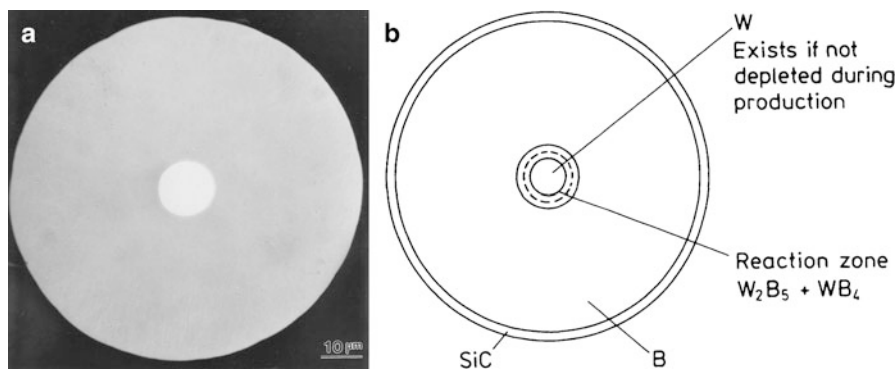


**Fig. 2.10** (a) Cross-section of a 100- $\mu\text{m}$ -diameter boron fiber. (b) Schematic of the cross-section of a boron fiber with SiC barrier layer

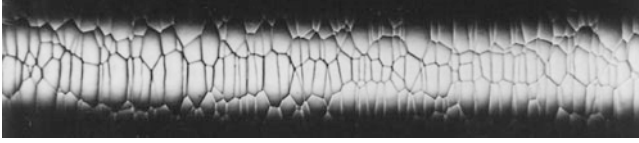


**Fig. 2.11** Characteristic corn-cob structure of boron fiber [from van Maaren et al. (1975), used with permission]. The fiber diameter is 142  $\mu\text{m}$

original 12.5  $\mu\text{m}$  (original tungsten wire diameter) to 17.5  $\mu\text{m}$ . The SiC coating shown in Fig. 2.10b is a barrier coating used to prevent any adverse reaction between B and the matrix, such as Al, at high temperatures. The SiC barrier layer is vapor deposited onto boron using a mixture of hydrogen and methylchlorosilane.

### 2.3.2.2 Morphology

The boron fiber surface shows a “corn-cob” structure consisting of nodules separated by boundaries (Fig. 2.11). The nodule size varies during the course of fabrication. In a very general way, the nodules start as individual nuclei on the substrate and then grow outward in a conical form until a filament diameter of 80–90  $\mu\text{m}$  is reached, above which the nodules seem to decrease in size. Occasionally, new cones may nucleate in the material, but they always originate at an interface with a foreign particle or inclusion.

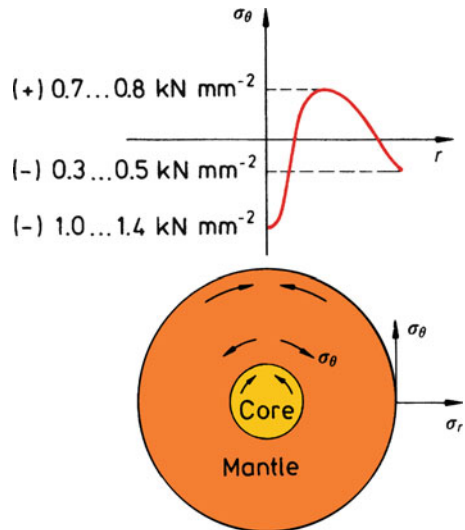
### 2.3.3 Residual Stresses

Boron fibers have inherent residual stresses that have their origin in the process of chemical vapor deposition. Growth stresses in the nodules of boron, stresses induced by the diffusion of boron into the tungsten core, and stresses generated by the difference in the coefficient of expansion of deposited boron and tungsten boride core, all contribute to the residual stresses and thus can have a considerable influence on the fiber mechanical properties. The residual stress pattern across the transverse section of a boron fiber is shown in Fig. 2.12 (Vega-Boggio and Vingsbo 1978). The compressive stresses on the fiber surface are due to the quenching action involved in pulling the fiber out from the chamber (Vega-Boggio and Vingsbo 1978). Morphologically, the most conspicuous aspect of these internal stresses is the frequently observed radial crack in the transverse section of these fibers. The crack runs from within the core to just inside the external surface. Some workers, however, doubt the preexistence of this radial crack (Krukonis 1977). They think that the crack appears during the process of boron fiber fracture.

### 2.3.4 Fracture Characteristics

It is well known that brittle materials show a distribution of strengths rather than a single value. Imperfections in these materials lead to stress concentrations much higher than the applied stress levels. Because the brittle material is not capable of deforming plastically in response to these stress concentrations, fracture ensues at one or more such sites. Boron fiber is indeed a very brittle material, and cracks originate at preexisting defects located at either the boron-core interface or the surface. Figure 2.13 shows the characteristic brittle fracture of a boron fiber and the radial crack. It is worth pointing out here that the radial crack does not extend all the way to surface of the fiber. This is because the surface layer of boron fiber is in compression; see Fig. 2.12. The surface defects in boron fiber stem from the nodular surface that results from the growth of boron cones. In particular, when a nodule coarsens due to an exaggerated growth around a contaminating particle, a crack can result from this large nodule and weaken the fiber.

**Fig. 2.12** Schematic of residual stress pattern across the transverse section of a boron fiber [from Vega-Boggio and Vingsbo (1978), used with permission]

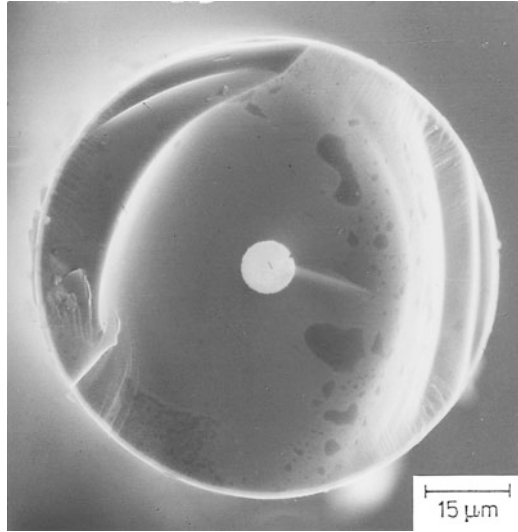


### 2.3.5 Properties and Applications of Boron Fibers

Many researchers have investigated the mechanical properties of boron fibers (Krukoniš 1977; Vega-Boggio and Vingsbo 1978; Galasso et al. 1967; Galasso and Paton 1966; DeBolt 1982; Wawner 1967; DiCarlo 1985). Due to the composite nature of the boron fiber, complex internal stresses and defects such as voids and structural discontinuities result from the presence of a core and the deposition process. Thus, one would not expect boron fiber to show the intrinsic



**Fig. 2.13** Fracture surface of a boron fiber showing a characteristically brittle fracture and a radial crack



strength of boron. The average tensile strength of boron fiber is 3–4 GPa, while its Young's modulus is between 380 and 400 GPa.

An idea of the intrinsic strength of boron can be obtained in a flexure test (Wawner 1967). In flexure, assuming the core and interface to be near the neutral axis, critical tensile stresses would not develop at the core or interface. Flexure tests on boron fibers lightly etched to remove any surface defects gave a strength of 14 GPa. Without etching, the strength was half this value. Table 2.3 provides a summary of the characteristics of boron fiber (DiCarlo 1985). Commercially produced 142- $\mu\text{m}$ -diameter boron fiber shows average tensile strength of 3.8 GPa. The tensile strength and fracture energy values of the as-received and some limited-production-run larger-diameter fibers showed improvement after chemical polishing, as shown in Table 2.3. Fibers showing strengths greater than 4 GPa had their fracture controlled by a tungsten boride core, while fibers with strengths of 4 GPa or less were controlled by fiber surface flaws. The high-temperature treatment, indicated in Table 2.3, improved the fiber properties by putting a permanent axial compressive strain in the sheath.

Boron has a density of 2.34  $\text{g}/\text{cm}^3$  (about 15 % less than that of aluminum). Boron fiber with a tungsten core has a density of 2.6  $\text{g}/\text{cm}^3$  for a fiber with 100  $\mu\text{m}$  diameter. Its melting point is 2,040  $^\circ\text{C}$ , and it has a thermal expansion coefficient of  $8.3 \times 10^{-6} \text{ }^\circ\text{C}^{-1}$  up to 315  $^\circ\text{C}$ .

Boron fiber composites are in use in a number of US military aircraft, notably the F-14 and F-15, and in the US space shuttle. They are also used for stiffening golf shafts, tennis rackets, bicycle frames, and in making repair patches for PMCs. A big advantage of boron fiber over other high performance fibers is their relatively better properties in compression. This stems from their larger diameter. A commercial product called Hy-Bor uses a mix of carbon and boron fibers in an epoxy matrix,

**Table 2.3** Strength properties of improved large-diameter boron fibers

Diameter ( $\mu\text{m}$ )	Treatment	Strength		Relative fracture energy
		Average <sup>a</sup> (GPa)	COV <sup>b</sup> (%)	
142	As-produced	3.8	10	1.0
406	As-produced	2.1	14	0.3
382	Chemical polish	4.6	4	1.4
382	Heat treatment plus polish	5.7	4	2.2

<sup>a</sup> Gauge length = 25 mm

<sup>b</sup> Coefficient of variation = standard deviation/average value

Source: Reprinted with permission from J Metals 37, No. 6, 1985, a publication of The Metallurgical Society, Warrendale PA

wherein improved properties in compression result because of the boron fibers. One big obstacle to the widespread use of boron fiber is its high cost compared to that of other fibers.

## 2.4 Carbon Fibers

Carbon is a very light element with a density equal to  $2.268 \text{ g/cm}^3$ . Carbon can exist in a variety of crystalline forms. Our interest here is in the so-called graphitic structure wherein the carbon atoms are arranged in the form of hexagonal layers. The other well-known form of carbon is the covalent diamond structure wherein the carbon atoms are arranged in a three-dimensional configuration with little structural flexibility. Another form of carbon is Buckminster Fullerene (or Bucky ball), with a molecular composition of  $\text{C}_{60}$  or  $\text{C}_{70}$ . One can also have carbon nanotubes, which are nothing but drawn out version of Buckyballs. Carbon in the graphitic form is highly anisotropic, with a theoretical Young's modulus in the layer plane being equal to about 1,000 GPa, while that along the *c*-axis is equal to about 35 GPa. The graphite structure (Fig. 2.14a) has a very dense packing in the layer planes. The lattice structure is shown more clearly with only lattice planes in Fig. 2.14b. As we know, the bond strength determines the modulus of a material. Thus, the high-strength bond between carbon atoms in the layer plane results in an extremely high modulus while the weak van der Waals-type bond between the neighboring layers results in a lower modulus in that direction. Consequently, almost all processing techniques of carbon fiber have the goal of obtaining a very high degree of preferred orientation of hexagonal planes along the fiber axis.

Carbon fibers of extremely high modulus can be made by carbonization of organic precursor fibers followed by graphitization at high temperatures. The organic precursor fiber, that is, the raw material for carbon fiber, is generally a special textile polymeric fiber that can be carbonized without melting. The precursor fiber, like any polymeric fiber, consists of long-chain molecules ( $0.1\text{--}1 \mu\text{m}$  when

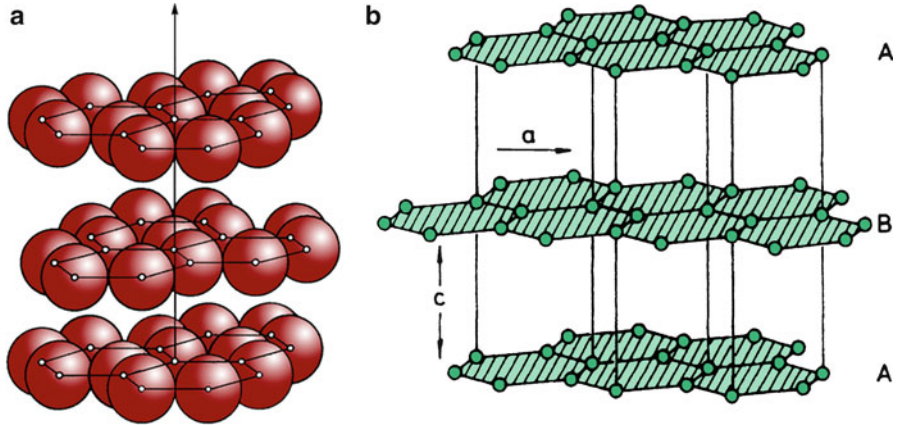


**Fig. 2.14** (a) Graphitic layer structure. The layers are shown not in contact for visual ease. (b) The hexagonal lattice structure of graphite

fully stretched) arranged in a random manner. Such polymeric fibers generally have poor mechanical properties and typically show rather large deformations at low stresses mainly because the polymeric chains are not ordered. A commonly used precursor fiber is polyacrylonitrile (PAN). Other precursor fibers include rayon and the ones obtained from pitches, polyvinyl alcohol, polyimides, and phenolics.

*Carbon fiber* is a generic term representing a family of fibers (Chawla 1981). As pointed out earlier, unlike the rigid diamond structure, graphitic carbon has a lamellar structure. Thus, depending on the size of the lamellar packets, their stacking heights, and the resulting crystalline orientations, one can obtain a range of properties. Most of the carbon fiber fabrication processes involve the following essential steps:

1. A *fiberization* procedure to make a precursor fiber. This generally involves wet-, dry-, or melt-spinning followed by some drawing or stretching.
2. A *stabilization* treatment that prevents the fiber from melting in the subsequent high-temperature treatments.
3. A thermal treatment called *carbonization* that removes most noncarbon elements.
4. An optional thermal treatment called *graphitization* that improves the properties of carbon fiber obtained in step 3.

It should be clear to the reader by now that in order to make a high-modulus fiber, one must improve the orientation of graphitic crystals or lamellas. This is achieved by various kinds of thermal and stretching treatments involving rather rigorous controls. If a constant stress were applied for a long time, for example, it would result in excessive fiber elongation and the accompanying reduction in area may lead to fiber fracture.

### 2.4.1 Processing

Back in late nineteenth century, Thomas Edison converted cellulose in the form of cotton fiber to carbon fiber. He was interested in using carbon fibers in incandescent lamps. In modern times, the field of high modulus carbon fibers for use in composites is said to have started when Shindo (1961) in Japan prepared high-modulus carbon fiber starting from PAN. He obtained a Young's modulus of about 170 GPa. In 1963, British researchers at Rolls Royce discovered that carbon fiber with a high elastic modulus could be obtained by incorporating a stretching treatment during the oxidation stage of processing. They obtained, starting from PAN, a carbon fiber with an elastic modulus of about 600 GPa. Since then, developments in the technology of carbon fibers have occurred in rapid strides. The minute details of the conversion processes from precursor fiber to a high-modulus carbon fiber continue to be proprietary secrets. All the methods, however, exploit the phenomenon of thermal decomposition of an organic fiber under well-controlled conditions of rate and time of heating, environment, and so on. Also, in all processes the precursor is stretched at some stage of pyrolysis to obtain the high degree of alignment of graphitic basal planes.

#### 2.4.1.1 Ex-PAN Carbon Fibers

Carbon fibers made from PAN are called *ex-PAN carbon fibers*. The PAN fibers are stabilized in air (a few hours at 250 °C) to prevent melting during the subsequent higher-temperature treatment. The fibers are kept under tension, i.e., they are prevented from contracting during this oxidation treatment. The white PAN fibers become black after oxidation. The black fibers obtained after this treatment are heated slowly in an inert atmosphere to 1,000–1,500 °C. Slow heating allows the high degree of order in the fiber to be maintained. The rate of temperature increase should be low so as not to destroy the molecular order in the fibers. The final optional heat treatment consists of holding the fibers for very short duration at temperatures up to 3,000 °C. This improves the fiber texture, i.e., the orientation of the basal planes and thus increases the elastic modulus of the fiber. Figure 2.15 shows, schematically, this PAN-based carbon fiber production process (Baker 1983). Typically, the carbon fiber yield is about 50 %.

Figure 2.16a shows the flexible PAN molecular structure. Note the all-carbon backbone. This structure is essentially that of polyethylene with a nitrile (CN) group on every alternate carbon atom. The structural changes occurring during the conversion of PAN to carbon fiber are as follows. The initial stretching treatment of PAN improves the axial alignment of the polymer molecules. During this oxidation treatment, the fibers are maintained under tension to keep the alignment of PAN while it transforms into rigid ladder polymer (Fig. 2.16b). In the absence of tensile stress in this step, a relaxation will occur, and the ladder polymer structure will become disoriented with respect to the fiber axis. After the stabilizing treatment,

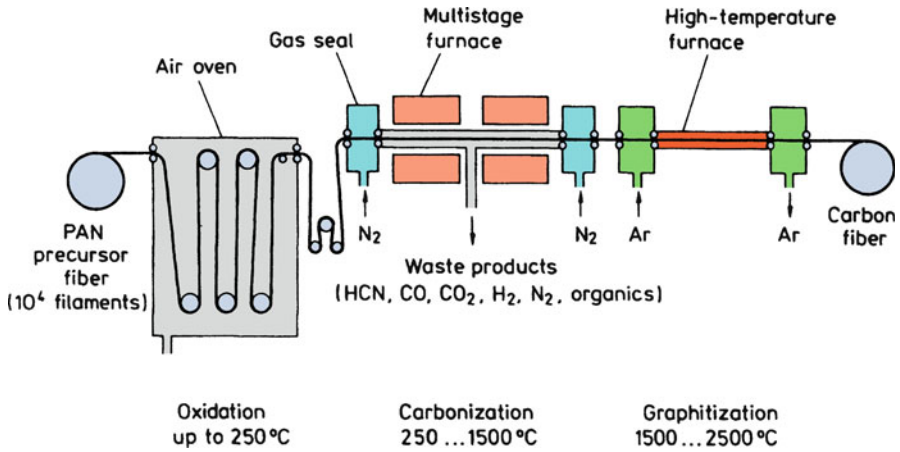


Fig. 2.15 Schematic of PAN-based carbon fiber production [reprinted with permission from Baker (1983)]

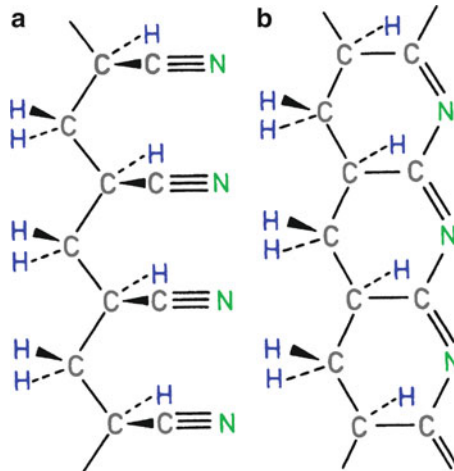


Fig. 2.16 (a) Flexible polyacrylonitrile molecule. (b) Rigid ladder (or oriented cyclic) molecule

the resulting ladder-type structure (also called *oriented cyclic structure*) has a high glass transition temperature so that there is no need to stretch the fiber during the next stage, which is carbonization. There are still considerable quantities of nitrogen and hydrogen present, which are eliminated as gaseous waste products during carbonization, that is, heating to 1,000–1,500 °C (Fig. 2.15). The carbon atoms remaining after this treatment are mainly in the form of a network of extended hexagonal ribbons, which has been called *turbostratic* graphite structure in the literature. Although these strips tend to align parallel to the fiber axis, the degree of order of

one ribbon with respect to another is relatively low. This can be improved further by heat treatment at still higher temperatures (up to 3,000 °C). This is the graphitization treatment (Fig. 2.15). The mechanical properties of the resultant carbon fiber may vary over a large range depending mainly on the temperature of the final heat treatment (Fig. 2.17) (Watt 1970). Hot stretching above 2,000 °C results in plastic deformation of carbon fibers, leading to an improvement in elastic modulus.

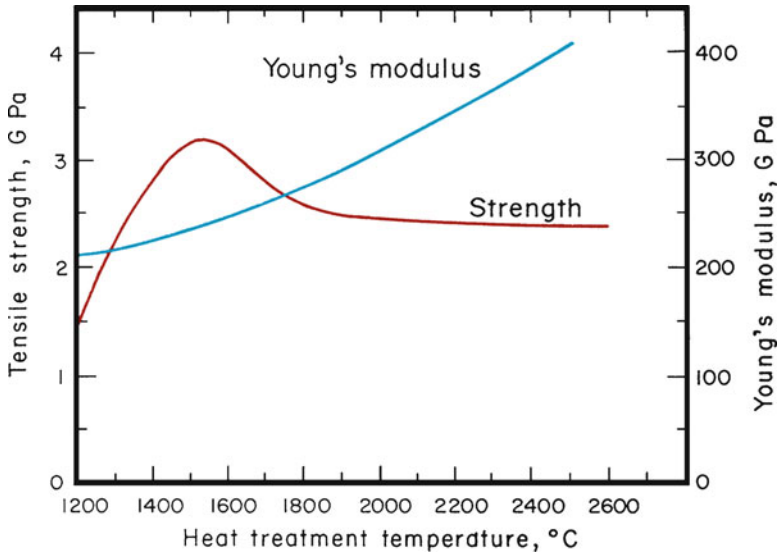


Fig. 2.17 Strength and elastic modulus of carbon fiber as a function of final heat treatment temperature [after Watt (1970), used with permission]

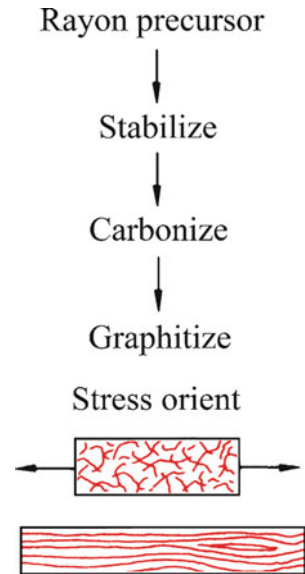
#### 2.4.1.2 Ex-Cellulose Carbon Fibers

Cellulose is a natural polymer that is frequently found in a fibrous form. In fact, cotton fiber, which is cellulosic, was one of the first to be carbonized. As mentioned above, Thomas Edison did that to obtain carbon filament for incandescent lamp. Cotton has the desirable property of decomposing before melting. It is not very suitable, however, for high-modulus carbon fiber manufacture because it has a rather low degree of orientation along the fiber axis, although it is highly crystalline. It is also not available as a tow of continuous filaments and is quite expensive. These difficulties have been overcome in the case of rayon fiber, which is made from wood pulp, a cheap source. The cellulose is extracted from wood pulp, and continuous filament tows are produced by wet spinning.

Rayon is a thermosetting polymer. The process used for the conversion of rayon into carbon fiber involves the same stages: fiberization, stabilization in a reactive atmosphere (air or oxygen, <400 °C), carbonization (<1,500 °C), and graphitization (>2,500 °C). Various reactions occur during the first stage, causing

extensive decomposition and evolution of  $H_2O$ ,  $CO$ ,  $CO_2$ , and tar. The stabilization is carried out in a reactive atmosphere to inhibit tar formation and improve yield (Bacon 1973). Chain fragmentation or depolymerization occurs in this stage. Because of this depolymerization, stabilizing under tension, as in the case of PAN precursor, does not work (Bacon 1973). The carbonization treatment involves heating to about  $1,000\text{ }^\circ\text{C}$  in nitrogen. Graphitization is carried out at  $2,800\text{ }^\circ\text{C}$  under stress. This orienting stress at high temperature results in plastic deformation via multiple-slip system operation and diffusion. Figure 2.18 shows the process schematically. The carbon fiber yield from rayon is between 15 and 30 % by weight, compared to a yield of about 50 % in the case of PAN precursors.

**Fig. 2.18** Schematic of rayon-based carbon fiber production [after Diefendorf and Tokarsky (1975), used with permission]



### 2.4.1.3 Ex-Pitch Carbon Fibers

There are various sources of pitch, but the three commonly used sources are polyvinyl chloride (PVC), petroleum asphalt, and coal tar. Pitch-based carbon fibers are attractive because of the cheap raw material, high yield of carbon fiber, and a highly oriented carbon fiber that can be obtained from mesophase pitch precursor fiber.

The same sequence of oxidation, carbonization, and graphitization is required for making carbon fibers from a pitch precursor. Orientation in this case is obtained by spinning. An isotropic but aromatic pitch is subjected to melt spinning at very high strain rates and quenched to give a highly oriented, pitch precursor fiber. This thermoplastic fiber is then oxidized to form a cross-linked structure that makes the fiber nonmelting. This is followed by carbonization and graphitization.

Commercial pitches are mixtures of various organic compounds with an average molecular weight between 400 and 600. Prolonged heating above 350 °C results in the formation of a highly oriented, optically anisotropic liquid crystalline phase (also called mesophase, Greek for intermediate phase). When observed under polarized light, anisotropic mesophase pitch appears as microspheres floating in isotropic pitch. The liquid crystalline mesophase pitch can be melt spun into a precursor for carbon fiber. The melt spinning process involves shear and elongation in the fiber axis direction, and thus a high degree of preferred orientation is achieved. This orientation can be further developed during conversion to carbon fiber. The pitch molecules (aromatics of low molecular weight) are stripped of hydrogen, and the aromatic molecules coalesce to form larger bidimensional molecules. Very high values of Young's modulus can be obtained. It should be appreciated that one must have the pitch in a state amenable to spinning in order to produce the precursor fiber, which is made infusible to allow carbonization to occur without melting. Thus, the pitches obtained from petroleum asphalt and coal tar need pretreatments. This pretreatment can be avoided in the case of PVC by means of a carefully controlled thermal degradation of PVC. Pitches are polydispersed systems, and thus they show a wide distribution of molecular weights, which can be adjusted by solvent extraction or distillation. The molecular weight controls the viscosity of the polymer melt and the melting range. Thus, it also controls the temperature and the spinning speed. Figure 2.19 shows the process of pitch-based carbon fiber manufacture starting from an isotropic pitch and a mesophase pitch (Diefendorf and Tokarsky 1975).

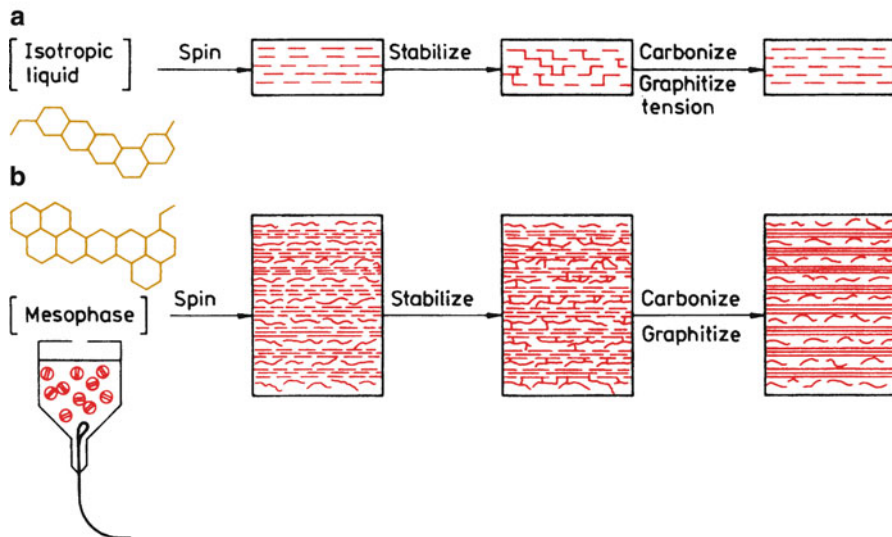


**Fig. 2.19** Schematic of pitch-based carbon fiber production: (a) isotropic pitch process, (b) mesophase pitch process [with permission from Diefendorf and Tokarsky (1975)]



### 2.4.2 Structural Changes Occurring During Processing

The thermal treatments for all precursor fibers serve to remove noncarbon elements in the form of gases. For this, the precursor fibers are stabilized to ensure that they decompose rather than melt. Generally, they become black after this treatment. Carbon fibers obtained after carbonization contain many “grown-in” defects because the thermal energy supplied at these low temperatures is not enough to break the already-formed carbon–carbon bonds. That is why these carbon fibers are very stable up to 2,500–3,000 °C when they change to graphite. The decomposition of the precursor fiber invariably results in a weight loss and a decrease in fiber diameter. The weight loss can be considerable—from 40 to 90 %, depending on the precursor and treatment (Ezekiel and Spain 1967). The external morphology of the fiber, however, is generally maintained. Thus, precursor fibers with transverse sections in the form of a kidney bean, dog bone, or circle maintain their form after conversion to carbon fiber. Figure 2.20 shows a scanning electron micrograph of a PAN-based carbon fiber. Note the surface markings that appear during the fiber drawing process.

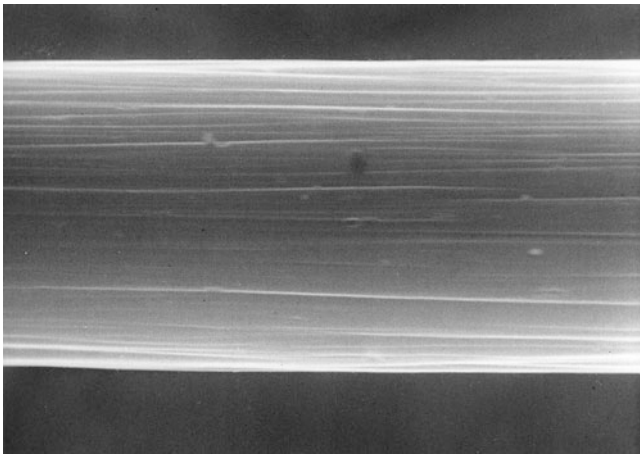
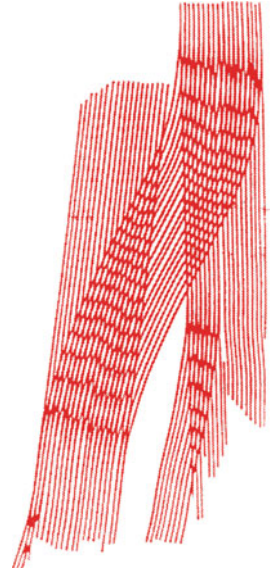


**Fig. 2.20** Scanning electron micrograph of PAN-based carbon fiber (fiber diameter is 8  $\mu\text{m}$ ). Note the surface markings that stem from the fiber drawing process

At the microscopic level, carbon fibers possess a rather heterogeneous microstructure. Not surprisingly, many workers (Diefendorf and Tokarsky 1975; Watt and Johnson 1969; Johnson and Tyson 1969; Perret and Ruland 1970; Bennett and Johnson 1978, 1979; Inal et al. 1980) have attempted to characterize the structure of carbon fibers, and one can find a number of models in the literature. There is a better understanding of the structure of PAN-based carbon fibers. Essentially, a carbon fiber consists of many graphitic lamellar ribbons oriented roughly parallel to the fiber axis with a complex interlinking of

layer planes both longitudinally and laterally. Based on high-resolution lattice fringe images of longitudinal and transverse sections in TEM, a schematic two-dimensional representation is given in Fig. 2.21 (Bennett and Johnson 1979), while a three-dimensional model is shown in Fig. 2.22 (Bennett and Johnson 1978). The structure is typically defined in terms of crystallite dimensions,  $L_a$  and  $L_c$  in directions  $a$  and  $c$ , respectively, as shown in Fig. 2.23. The degree of alignment and the parameters  $L_a$  and  $L_c$  vary with the graphitization temperature. Both  $L_a$  and  $L_c$  increase with increasing heat treatment temperature.

**Fig. 2.21** Two-dimensional representation of PAN-based carbon fiber [after Bennett and Johnson (1979), used with permission]



### 2.4.3 Properties and Applications

The density of the carbon fiber varies with the precursor and the thermal treatment given. It is generally in the range of 1.6–2.0 g/cm<sup>3</sup>. Note that the density of the carbon fiber is more than that of the precursor fiber; the density of the precursor is generally between 1.14 and 1.19 g/cm<sup>3</sup> (Bennett et al. 1983). There are always flaws of various kinds present, which may arise from impurities in the precursors or may simply be the misoriented layer planes. A mechanism of tensile failure of carbon fiber based on the presence of misoriented crystallites is shown in Fig. 2.23 (Bennett et al. 1983). Figure 2.23a shows a misoriented crystallite linking two crystallites parallel to the fiber axis. Under the action of applied stress, basal plane rupture occurs in the misoriented crystallite in the  $L_c$  direction, followed by crack development along  $L_a$  and  $L_c$  (Fig. 2.23b). Continued stressing causes complete failure of the misoriented crystallite (Fig. 2.23c). If the crack size is greater than the critical size in the  $L_a$  and  $L_c$  directions, catastrophic failure results.



**Fig. 2.22** Three-dimensional representation of PAN-based carbon fiber [from Bennett and Johnson (1978), used with permission]

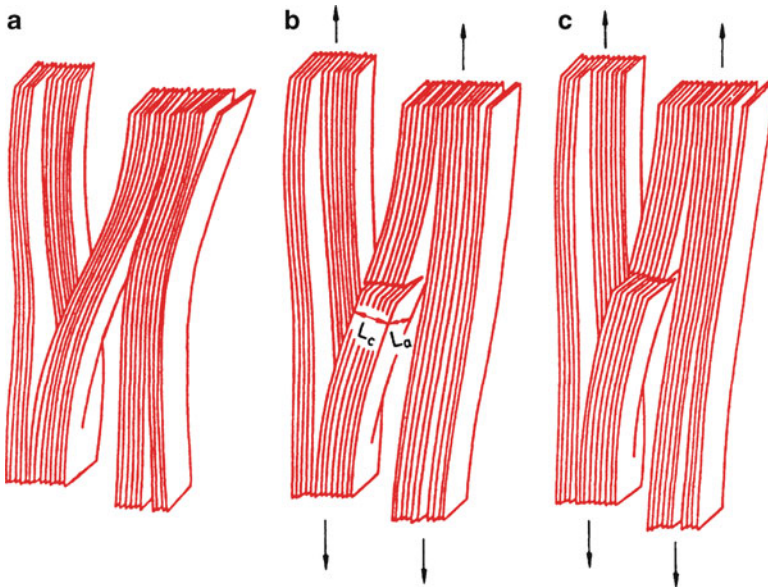
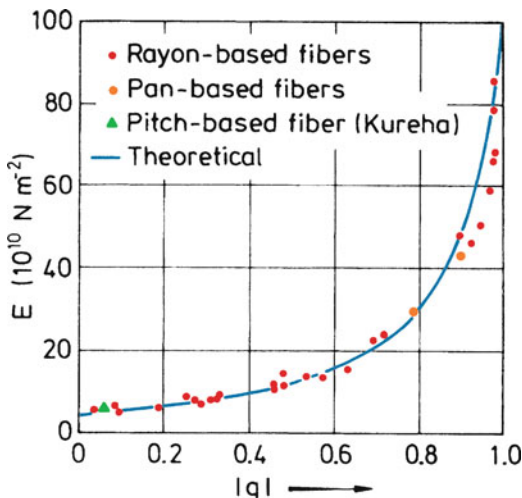


**Fig. 2.23** Model for tensile failure of carbon fiber: (a) a misoriented crystallite linking two crystallites parallel to the fiber axis, (b) basal plane rupture under the action of applied stress, (c) complete failure of the misoriented crystallite [from Bennett et al. (1983), used with permission]

As mentioned earlier, the degree of order, and consequently the modulus in the fiber axis direction, increases with increasing graphitization temperature. Fourdeux et al. (1971) measured the preferred orientation of various carbon fibers and plotted the Young's modulus of the carbon fibers obtained by different precursors against an orientation parameter,  $q$  (Fig. 2.24). The absolute value of this parameter,  $|q|$  has a value of 1 for perfect orientation and zero for the isotropic case. In Fig. 2.24 we have plotted the absolute value of  $q$ . Note also that the modulus has been corrected for porosity. The theoretical curve fits the experimental data very well.

**Fig. 2.24** Variation of longitudinal Young's modulus for various carbon fibers with the degree of preferred orientation. The value of the orientation parameter,  $q$ , is 1 for perfect orientation and zero for the isotropic case [from Fourdeux et al. (1971), used with permission]



Even among the PAN carbon fibers, we can have a series of carbon fibers: for example, high tensile strength but medium Young's modulus (HT) fiber (200–300 GPa); high Young's modulus (HM) fiber (400 GPa); extra- or superhigh tensile strength (SHT); and superhigh modulus type (SHM) carbon fibers. The mesophase pitch-based carbon fibers show rather high modulus but low strength levels (2 GPa). Not unexpectedly, the HT-type carbon fibers show a much higher strain-to-failure value than the HM type. The mesophase pitch-based carbon fibers are used for reinforcement, while the isotropic pitch-based carbon fibers (very low modulus) are more frequently used as insulation and fillers. Table 2.4 compares the properties of some common carbon fibers and graphite monocrystal (Singer 1979). For high-temperature applications involving carbon fibers, it is important to take into account the variation of inherent oxidation resistance of carbon fibers with modulus. Figure 2.25 shows that the oxidation resistance of carbon fiber increases with the modulus value (Riggs 1985). The modulus, as we know, increases with the final heat treatment temperature during processing.

We note from Table 2.4 that the carbon fibers produced from various precursor materials are fairly good electrical conductors. Although this led to some work toward a potential use of carbon fibers as current carriers for electrical power transmission

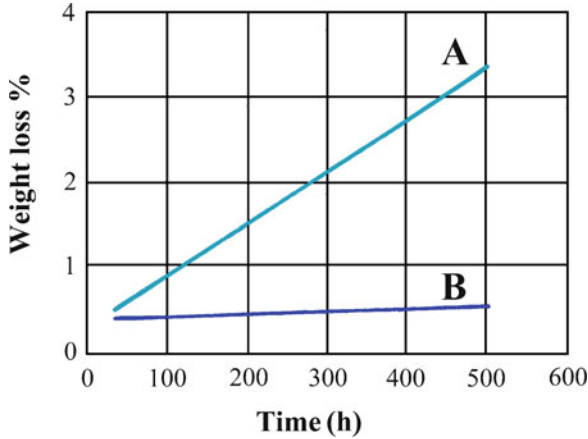


**Fig. 2.25** Oxidation resistance, measured as weight loss in air at 350 °C, of carbon fibers having different moduli: (A) Low modulus Celion 3000 (240 GPa) and (B) High modulus Celion G-50 (345 GPa) [after Riggs JP (1985) Encyclopedia of polymer science and engineering, 2e, vol 2, John Wiley and Sons, New York, reprinted with permission]

**Table 2.4** Comparison of properties of different carbon fibers

Precursor	Density (g/cm <sup>3</sup> )	Young's modulus (GPa)	Electrical resistivity (10 <sup>-4</sup> Ω cm)
Rayon <sup>a</sup>	1.66	390	10
Polyacrylonitrile <sup>b</sup> (PAN)	1.74	230	18
Pitch (Kureha)			
LT <sup>c</sup>	1.6	41	100
HT <sup>d</sup>	1.6	41	50
Mesophase pitch <sup>e</sup>			
LT	2.1	340	9
HT	2.2	690	1.8
Single-crystal <sup>f</sup> graphite	2.25	1,000	0.40

<sup>a</sup>Union Carbide, Thornel 50

<sup>b</sup>Union Carbide, Thornel 300

<sup>c</sup>LT low-temperature heat-treated

<sup>d</sup>HT high-temperature heat-treated

<sup>e</sup>Union Carbide type P fibers

<sup>f</sup>Modulus and resistivity are in-plane values

Source: Adapted with permission from Singer (1979)

(Murday et al. 1984), it also caused extreme concern in many quarters. The reason for this concern is that if the extremely fine carbon fibers accidentally become airborne (during manufacture or service) they can settle on electrical equipment and cause short circuiting. An interesting characteristic of ex-mesophase pitch carbon fiber is the

extremely high thermal conductivity it can have. Ex-pitch carbon fibers with a suitably oriented microstructure can have thermal conductivity as high as 1,100 W/mK. The figure for an ex-PAN carbon fiber is generally less than 50 W/mK.

Anisotropic as the carbon fibers are, they have two principal coefficients of thermal expansion, namely, longitudinal or parallel to the fiber axis,  $\alpha_l$  and transverse or perpendicular to the fiber axis,  $\alpha_t$ . Typical values of the expansion coefficients are

$$\alpha_l \approx 5.5 \text{ to } 8.4 \times 10^{-6} \text{ K}^{-1},$$

$$\alpha_t \approx -0.5 \text{ to } -1.3 \times 10^{-6} \text{ K}^{-1}.$$

Compressive strength of carbon fibers is about half their tensile strength! Still, they are an order of magnitude better than aramid-type fibers (see Sect. 2.5).

Carbon fibers are used in a variety of applications in the aerospace and sporting goods industries. Cargo bay doors and booster rocket casings in the US space shuttle are made of carbon fiber reinforced epoxy composites. Modern commercial aircraft such as Boeing 787 (Dreamliner) has fuselage and wings made of carbon fiber/epoxy composites. With the ever decreasing price of carbon fibers, applications of carbon fibers in other areas have also increased, for example, various machinery items such as turbine, compressor, and windmill blades and flywheels; in the field of medicine the applications include both equipment and implant materials (e.g., ligament replacement in knees and hip joint replacement). We discuss these in more detail in Chap. 5.

## 2.5 Organic Fibers

In general, polymeric chains assume a random coil configuration, i.e., they have the so-called cooked-spaghetti structure (see Chap. 3). In this random coil structure, the macromolecular chains are neither aligned in one direction nor stretched out. Thus, they have predominantly weak van der Waals interactions rather than strong covalent interactions, resulting in a low strength and stiffness. Because the covalent carbon-carbon bond is very strong, one would expect that linear chain polymers, such as polyethylene, would be potentially very strong and stiff. Conventional polymers show a Young's modulus,  $E$ , of about 10 GPa or less. Highly drawn polymers with a Young's modulus of about 70 GPa can be obtained easily. However, if one wants strong and stiff organic fibers, one must obtain not only oriented molecular chains but oriented *and* fully extended chains. Thus, in order to obtain high-stiffness and high-strength polymers, we must extend these polymer chains and pack them in a parallel array. The orientation of these polymer chains with respect to the fiber axis and the manner in which they fit together (i.e., order or crystallinity) are controlled by their chemical nature and the processing route. The case of molecular chain orientation without high molecular extension is shown in Fig. 2.26a while chain orientation with high molecular extension is depicted

in Fig. 2.26b. It is the chain structure shown in Fig. 2.26b, i.e., molecular chain orientation coupled with molecular chain extension, which is needed for high stiffness and high strength. To get a Young's modulus value greater than 70 GPa, one needs rather high draw ratios, i.e., a very high degree of elongation must be carried out under such conditions that macroscopic elongation results in a corresponding elongation at a molecular level. It turns out that the Young's modulus,  $E$ , of a polymeric fiber increases linearly with the deformation ratio (draw ratio in tensile drawing or die drawing and extrusion ratio in hydrostatic extrusion). The drawing behavior of a polymer is a sensitive function of (1) its molecular weight and molecular weight distribution and (2) deformation conditions (temperature and strain rate). Too low a drawing temperature produces voids, while too high a drawing temperature results in flow drawing, i.e., the macroscopic elongation of the material does not result in a molecular alignment, and consequently, no stiffness enhancement results. An oriented and extended macromolecular chain structure, however, is not easy to achieve in practice.

Nevertheless, considerable progress in this area was made during the last quarter of the twentieth century. Organic fibers, such as aramid and polyethylene, possessing high strength and modulus are the fruits of this realization. Two very different approaches have been taken to make high-modulus organic fibers. These are:

1. Process the conventional flexible-chain polymers in such a way that the internal structure takes a highly oriented and extended-chain arrangement. Structural modification of "conventional" polymers such as high-modulus polyethylene

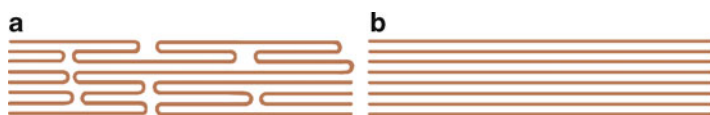


**Fig. 2.26** Two types of molecular orientation: (a) oriented *without* high molecular extension and (b) oriented *with* high molecular extension [from Barham and Keller (1985), used with permission]

was developed by choosing appropriate molecular weight distributions, followed by drawing at suitable temperatures to convert the original folded-chain structure into an oriented, extended chain structure.

2. The second, radically different, approach involves synthesis, followed by extrusion of a new class of polymers, called liquid crystal polymers. These have a rigid-rod molecular chain structure. The liquid crystalline state, as we shall see, has played a very significant role in providing highly ordered, extended chain fibers.

These two approaches have resulted in two commercialized high-strength and high-stiffness fibers, polyethylene and aramid. Next, we describe the processing, structure, and properties of these two fibers.

### 2.5.1 Oriented Polyethylene Fibers

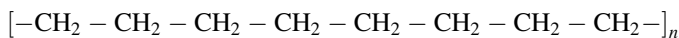
The ultrahigh-molecular-weight polyethylene (UHMWPE) fiber is a highly crystalline fiber with very high stiffness and strength. This results from some innovative processing and control of the structure of polyethylene.

#### 2.5.1.1 Processing of Polyethylene Fibers

Drawing of melt crystallized polyethylene (molecular mass between  $10^4$  and  $10^5$ ) to very high draw ratios can result in moduli of up to 70 GPa. Tensile drawing, die drawing, or hydrostatic extrusion can be used to obtain the high permanent or plastic strains required to obtain a high modulus. It turns out that modulus is dependent on the draw ratio but independent of how the draw ratio is obtained (Capaccio et al. 1979). In all these drawing processes, the polymer chains become merely oriented without undergoing molecular extension, and we obtain the kind of structure shown in Fig. 2.26a. Later developments led to solution and gel spinning of very high molecular weight polyethylene ( $>10^6$ ) with moduli as high as 200 GPa. The gel spinning method of making polyethylene fibers has become technologically and commercially most successful. Pennings and coworkers (Kalb and Pennings 1980; Smook and Pennings 1984) made high-modulus polyethylene fiber by solution spinning. Their work was preceded by Smith and Lemstra (1976), who made polyethylene fiber by gel spinning. The gel spinning process of making polyethylene was industrialized in the 1980s. *Gels* are swollen networks in which crystalline regions form the network junctions. An appropriate polymer solution is converted into gel, which is drawn to give the fiber. At least three commercial firms produce oriented polyethylene fiber using similar techniques; *Dyneema*, *Spectra*, *Tekmilon* are the trade names of these UHMWPE fibers. Next, we describe the gel spinning process of making the high-stiffness polyethylene fiber.

#### 2.5.1.2 Gel Spinning of Polyethylene Fiber

Polyethylene (PE) is a particularly simple, linear macromolecule, with the following chemical formula



Thus, compared to other polymers, it is easier to obtain an extended and oriented chain structure in polyethylene. High-density polyethylene (HDPE) is preferred to other types of polyethylene because HDPE has fewer branch points along its backbone and a high degree of crystallinity. The characteristics of linearity and crystallinity are important from the point of getting a high degree of orientational order and obtaining an extended chain structure in the final fiber.



Figure 2.27 provides a flow diagram of the gel spinning process for making the high-modulus polyethylene fiber. Different companies use different solvents, such as decalin, paraffin oil, and paraffin wax, to make a dilute (5–10 %) solution of polymer in the appropriate solvent at about 150 °C. A dilute solution is important in that it allows for a lesser chain entanglement, which makes it easier for the final fiber to be highly oriented. A polyethylene gel is produced when the solution coming out of the spinneret is quenched by air. The as-spun gelled fiber enters a cooling bath. At this stage, the fiber is thought to have a structure consisting of folded chain lamellae with solvent between them and a swollen network of entanglements. These entanglements allow the as-spun fiber to be drawn to very high draw ratios, which can be as high as 200. The maximum draw ratio is related to the average distance between the entanglements, i.e., the solution concentration. The gelled fibers are drawn at 120 °C. One problem with this gel route is the rather low spinning rates of 1.5 m/min. At higher rates, the properties obtained are not very good (Kalb and Pennings 1980; Smook and Pennings 1984).

### 2.5.1.3 Structure and Properties of Polyethylene Fiber

The unit cell of a single crystal (orthorhombic) of polyethylene has the dimensions of 0.741, 0.494, and 0.255 nm. There are four carbon and eight hydrogen atoms per

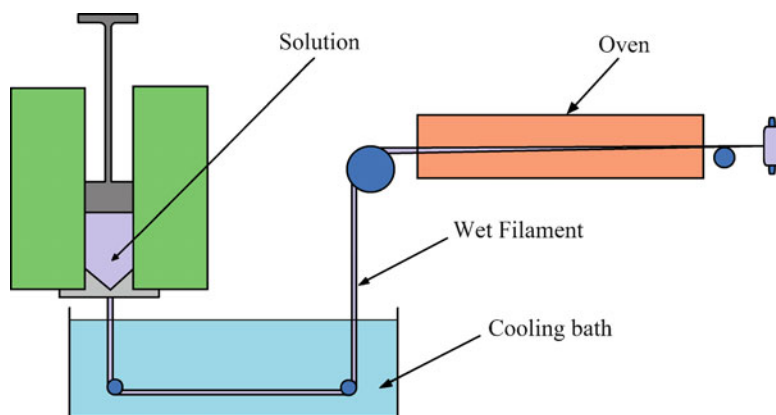


Fig. 2.27 Gel spinning process for making the high-modulus polyethylene fiber concentration

Table 2.5 Properties of polyethylene fibers<sup>a</sup>

Property	Spectra 900	Spectra 1000
Density (g/cm <sup>3</sup> )	0.97	0.97
Diameter (μm)	38	27
Tensile strength (GPa)	2.7	3.0
Tensile modulus (GPa)	119	175
Tensile strain to fracture (%)	3.5	2.7

<sup>a</sup>Manufacturer's data; indicative values

unit cell. One can compute the theoretical density of polyethylene, assuming a 100 % single-crystal polyethylene. If one does that, the theoretical density of polyethylene comes out to be  $0.9979 \text{ g/cm}^3$ ; of course, in practice, one can only tend toward this theoretical value. As it turns out, the highly crystalline, oriented and extended chain UHMWPE fiber has a density of  $0.97 \text{ g/cm}^3$ , which is very near the theoretical value. Thus, polyethylene fiber is very light; in fact, it is lighter than water and thus floats on water. Properties of some commercially available polyethylene fibers are summarized in Table 2.5.

Its strength and modulus are slightly lower than those of aramid fibers but on a per-unit-weight basis, i.e., specific property values are about 30–40 % higher than those of aramid. As is true of most organic fibers, both polyethylene and aramid fibers must be limited to low-temperature (lower than  $150 \text{ }^\circ\text{C}$ ) applications.

Another effect of the high degree of chain alignment in these fibers is their super smooth surface. This is manifested when they are put in a polymeric matrix to form a fiber reinforced composite. High-modulus polyethylene fibers, such as Spectra and Dyneema, are hard to bond with any polymeric matrix. Some kind of surface treatment must be given to the polyethylene fiber to bond with resins such as epoxy and PMMA. By far, the most successful surface treatment involves a cold gas (such as air, ammonia, or argon) plasma (Kaplan et al. 1988). A plasma consists of gas molecules in an excited state, i.e., highly reactive, dissociated molecules. When the polyethylene, or any other fiber, is treated with a plasma, surface modification occurs by the removal of any surface contaminants and highly oriented surface layers, the addition of polar and functional groups on the surface, and the introduction of surface roughness; all these factors contribute to an enhanced fiber/matrix interfacial strength (Biro et al. 1992; Brown et al. 1992; Hild and Schwartz 1992a, b; Kaplan et al. 1988; Li et al. 1992). Exposure to the plasma for just a few minutes is enough.

Polyethylene fiber (the gel spun UHMWPE variety) is 90–95 % crystalline and has a density of  $0.97 \text{ g/cm}^3$ . There is a linear relationship between density and crystallinity for polyethylene. A 100 % crystalline polyethylene will have a theoretical density, based on an orthorhombic unit cell, of about  $1 \text{ g/cm}^3$ . A totally amorphous polyethylene (0 % crystallinity) will have a density of about  $0.85 \text{ g/cm}^3$ . Raman spectroscopy has been used to study the deformation behavior of polyethylene fiber. Creep properties of these fibers are not very good, Spectra 1000 has better creep properties than Spectra 900. It should be mentioned that although plasma treatment, in general, improves the interfacial adhesion between the fiber and the matrix, it does result in some deterioration of the mechanical properties of the fiber.

### 2.5.2 Aramid Fibers

*Aramid fiber* is a generic term for a class of synthetic organic fibers called aromatic polyamide fibers. The US Federal Trade Commission gives a good definition of an

aramid fiber as “a manufactured fiber in which the fiber-forming substance is a long-chain synthetic polyamide in which at least 85 % of the amide linkages are attached directly to two aromatic rings.” Well-known commercial names of aramid fibers include Kevlar and Nomex (Du Pont) and Twaron (Teijin Aramid). Teijinconex and Technora are two other commercially available fibers from Teijin. *Nylon* is a generic name for any long-chain polyamide. Aramid fibers such as Nomex or Kevlar, however, are ring compounds based on the structure of benzene as opposed to the linear compounds used to make nylon. The basic difference between Kevlar and Nomex is that Kevlar has *para*-oriented aromatic rings, i.e., its basic unit is a symmetric molecule, with bonds from each aromatic ring being parallel, while Nomex is *meta*-oriented, with bonds at 120-degree angles to each other. Teijinconex is similar to Nomex while Twaron is similar to Kevlar. Technora is a copolyamide. The basic chemical structure of aramid fibers consists of oriented *para*-substituted aromatic units, which makes them rigid rodlike polymers. The rigid rodlike structure results in a high glass transition temperature and poor solubility, which makes fabrication of these polymers, by conventional drawing techniques, difficult. Instead, they are spun from liquid crystalline polymer solutions by dry jet–wet spinning, as described in the next section.

### 2.5.2.1 Processing of Aramid Fibers

Processing of aramid fibers involves solution-polycondensation of diamines and diacid halides at low temperatures. Hodd and Turley (1978), Morgan (1979), and Magat (1980) have given simplified accounts of the theory involved in the fabrication of aramid fibers.

The most important point is that the starting spinnable solutions that give high-strength and high-modulus fibers have liquid crystalline order. Figure 2.28 shows schematically various states of a polymer in solution. Figure 2.28a shows two-dimensional, linear, flexible chain polymers in solution. These are called *random coils*, as the figure suggests. If the polymer chains can be made of rigid units, that is,

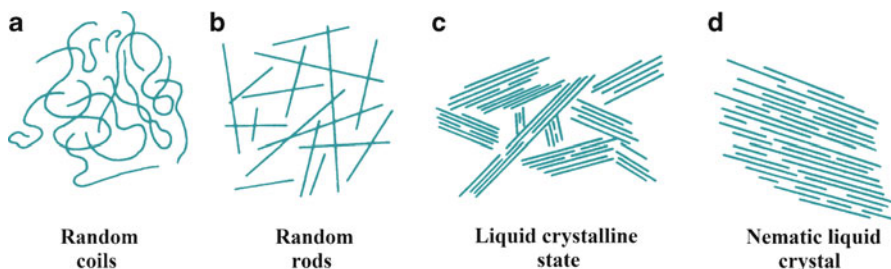


**Fig. 2.28** Various states of polymer in solution: (a) two-dimensional, linear, flexible chains (random coils), (b) random array of rods, (c) partially ordered liquid crystalline state, and (d) nematic liquid crystal (randomly distributed parallel rods)

rodlike, we can represent them as a random array of rods (Fig. 2.28b). Any associated solvent may contribute to the rigidity and to the volume occupied by each polymer molecule. It is easy to see that with increasing concentration of rodlike molecules, one can dissolve more polymer by forming regions of partial order, that is, regions in which the chains form a parallel array. This partially ordered state is called a *liquid crystalline state* (Fig. 2.28c). When the rodlike chains become approximately arranged parallel to their long axes, but their centers remain unorganized or randomly distributed, we have what is called a *nematic liquid crystal* (Fig. 2.28d). It is this kind of order that is found in the extended-chain polyamides.

Liquid crystal solutions, because of the presence of the ordered domains, are optically anisotropic, that is, they show the phenomenon of *birefringence*. Birefringence, also known as double refraction, is the phenomenon of splitting of a ray of light into two rays when it passes through certain types of material, depending on the polarization of the light. Figure 2.29 shows the anisotropic Kevlar aramid and sulfuric acid solution at rest between crossed polarizers. Note the parallel arrays of ordered polymer chains in the liquid crystalline state, which become even more ordered when these solutions are subjected to shear as, for example, in extruding through a spinneret hole. It is this inherent property of liquid crystal solutions that is exploited in the manufacture of aramid fibers. This alignment of polymer crystallites along the fiber axis results in the characteristic fibrillar structure of aramid fibers. *Para*-oriented aromatic polyamides form liquid crystal solutions under certain conditions of concentration, temperature, solvent, and molecular weight. This can be represented in the form of a phase diagram. As an example, Fig. 2.30a shows a phase diagram of the system poly-*p*-benzamide in tetramethylurea-LiCl solutions (Magat 1980). The region marked anisotropic represents the liquid crystalline state. Only under certain conditions do we get this desirable anisotropic state. There also occurs an anomalous relationship between viscosity and polymer concentration in liquid crystal solutions. Initially, an increase in viscosity occurs as the concentration of polymer in solution increases, as it would in any ordinary polymer solution. At a critical point where it starts assuming an anisotropic liquid crystalline shape, a sharp drop in the viscosity occurs; see Fig. 2.30b. This drop in viscosity of liquid crystal polymers at a critical concentration was predicted by Flory (1956). The drop in viscosity occurs due to the formation of a lyotropic nematic structure. The liquid crystalline regions act like dispersed particles and contribute very little to viscosity of the solution. With increasing polymer concentration, the amount of liquid crystalline phase increases up to a point after which the viscosity tends to rise again. There are other requirements for forming a liquid crystalline solution from aromatic polyamides. The molecular weight must be greater than some minimum value and the solubility must exceed the critical concentration required for liquid crystallinity. Thus, starting from liquid crystalline spinning solutions containing highly ordered arrays of extended polymer chains, we can spin fibers directly into an extremely oriented, chain-extended form. These as-spun fibers are quite strong and, because the chains are highly extended and oriented, the use of conventional drawing techniques becomes optional.

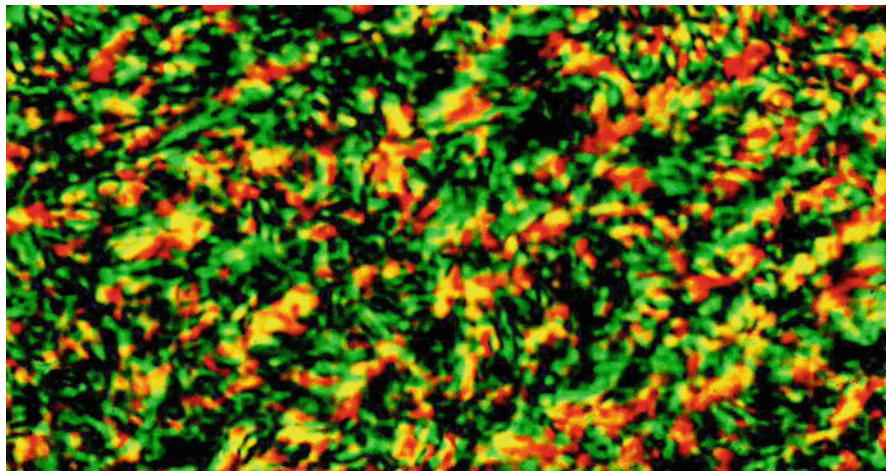
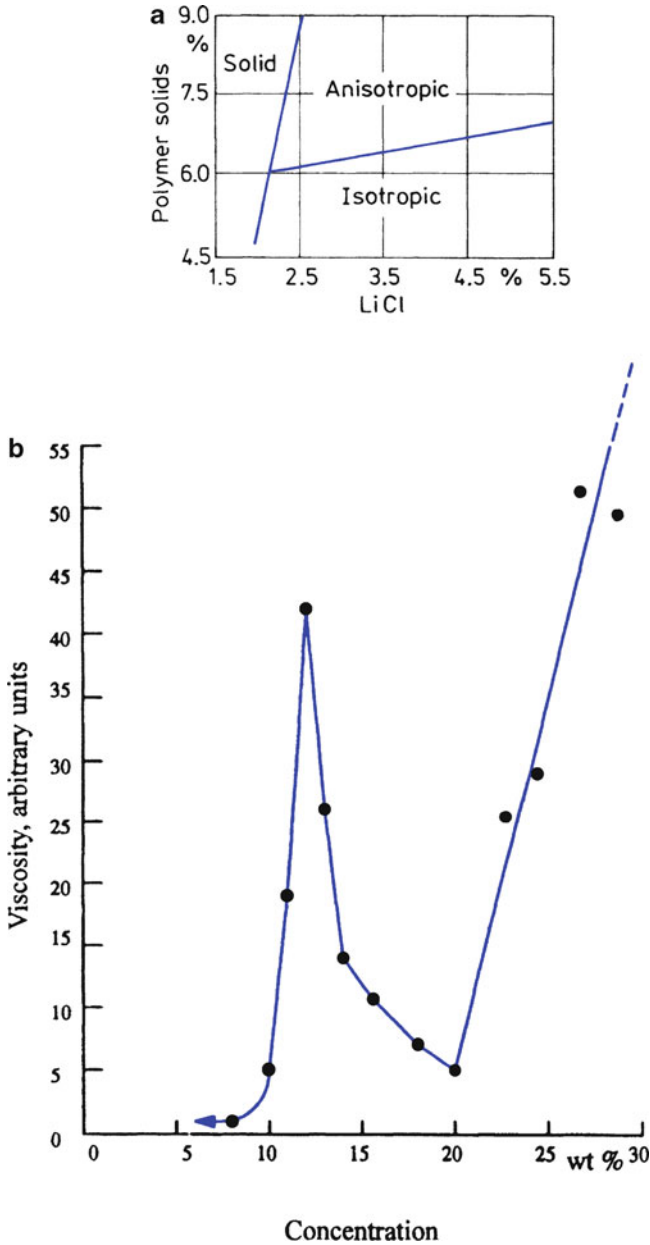


Fig. 2.29 Anisotropic Kevlar aramid and sulfuric acid solution at rest between crossed polarizers [courtesy of Du Pont Co.]

*Para*-oriented rigid diamines and dibasic acids give polyamides that yield, under appropriate conditions of solvent, polymer concentration, and polymer molecular weight, the desired nematic liquid crystal structure. One would like to have, for any solution spinning process, a high molecular weight in order to have improved mechanical properties, a low viscosity to easily spin the fiber, and a high polymer concentration for high yield. For *para*-aramid, poly-*p*-phenylene terephthalamide (PPTA), the nematic liquid crystalline state is obtained in 100 % sulfuric acid solvent at a polymer concentration of about 20 %. That is, to dissolve PPTA we need concentrated sulfuric acid as the solvent. In industry, this solution is often referred to as the *dope*.

For aramid fibers, the dry jet–wet spinning method is used. The process is illustrated in Fig. 2.31. Solution-polycondensation of diamines and diacid halides at low temperatures (near 0 °C) gives the aramid forming polyamides. Low temperatures are used to inhibit any by-product generation and promote linear polyamide formation. The resulting polymer is pulverized, washed, and dried; mixed with concentrated H<sub>2</sub>SO<sub>4</sub>; and extruded through a spinneret at about 100 °C. The jets from the orifices pass through about 1 cm of air layer before entering a cold water (0–4 °C) bath. The fiber solidifies in the air gap, and the acid is removed in the coagulation bath. The spinneret capillary and air gap cause rotation and alignment of the domains, resulting in highly crystalline and oriented as-spun fibers. The air gap also allows the dope to be at a higher temperature than is possible without the air gap. The higher temperature allows a more concentrated spinning solution to be used, and higher spinning rates are possible. Spinning rates of several hundred meters per minute are not unusual. Figure 2.32 compares the dry jet–wet spinning method used with nematic liquid crystals and the spinning of a conventional polymer. The oriented chain structure, together with molecular extension, is achieved with dry jet–wet spinning. The conventional wet or dry spinning gives



**Fig. 2.30** (a) Phase diagram of poly-*p*-benzamide in tetramethylurea–LiCl solutions. Note that the anisotropic state is obtained under certain conditions [with permission from Magat (1980)] (b) Viscosity vs. polymer concentration in solution. A sharp drop in viscosity occurs when the solution starts becoming anisotropic liquid crystal [after Kwolek and Yang (1993)]

**Fig. 2.31** The dry jet–wet spinning process of producing aramid fibers

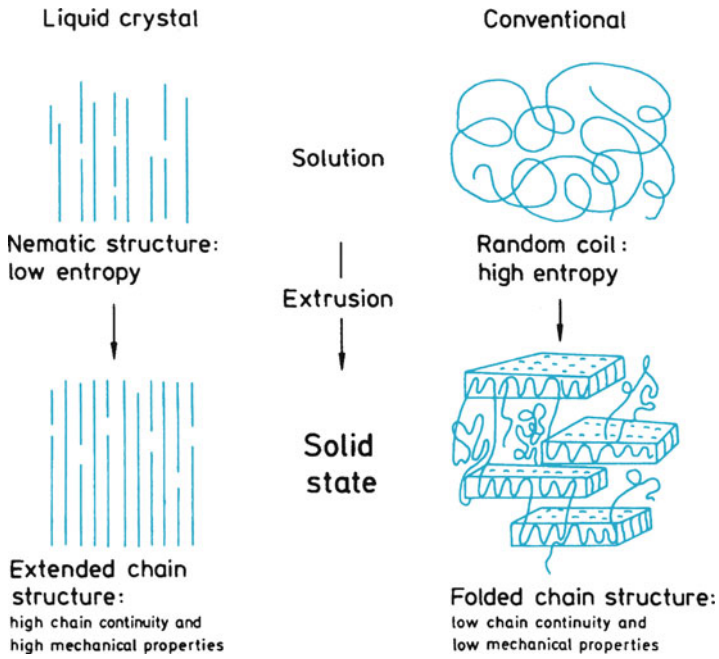
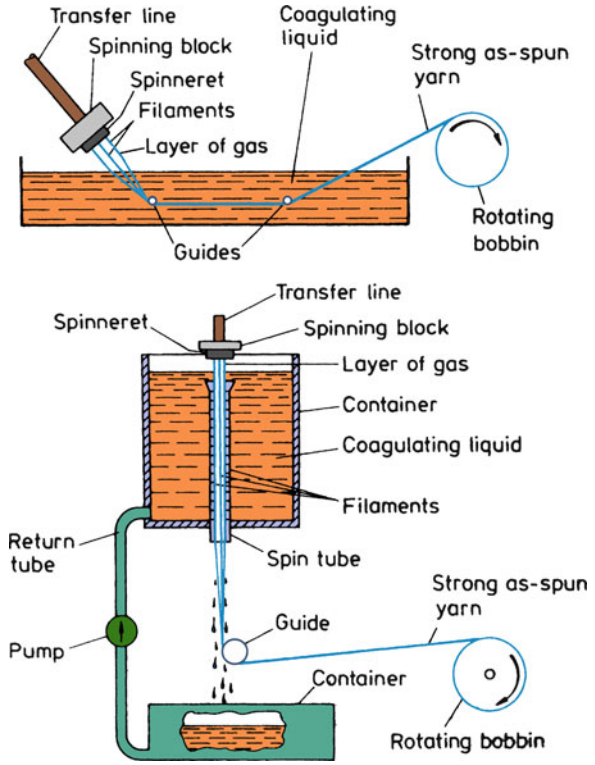


**Fig. 2.32** Comparison of dry jet–wet spinning of nematic liquid crystalline solution and conventional spinning of a polymer [reprinted from Jaffe and Jones (1985), p 349, courtesy of Marcel Dekker, Inc.]

precursors that need further processing for a marked improvement in properties (Jaffe and Jones 1985). The as-spun fibers are washed in water, wound on a bobbin, and dried. Fiber properties are modified by the use of appropriate solvent additives, by changing the spinning conditions, and by means of some post-spinning heat treatments, if necessary.

The aramid fiber known as Technora (formerly HM-50) is made slightly differently from the liquid crystal route just described. Three monomers—terephthalic acid, *p*-phenylenediamine (PDA), and 3,4-diamino diphenyl ether—are used. The ether monomer provides more flexibility to the backbone chain, which results in a fiber that has slightly better compressive properties than PPTA aramid fiber made via the liquid crystal route. An amide solvent with a small amount of salt (calcium chloride or lithium chloride) is used as a solvent (Ozawa et al. 1978). The polymerization is done at 0–80 °C in 1–5 h and with a polymer concentration of 6–12 %. The reaction mixture is spun from a spinneret into a coagulating bath containing 35–50 % CaCl<sub>2</sub>. Draw ratios between 6 and 10 are used.

### 2.5.2.2 Structure of Aramid Fibers

Kevlar aramid fiber is the most studied of all aramid fibers. Thus, our description of structure will mostly be from the work done on Kevlar, but it applies to Twaron as well. The chemical formula of aramid is given in Fig. 2.33. Chemically, the Kevlar- or Twaron-type aramid fiber is poly (*p*-phenyleneterephthalamide), which is a polycondensation product of terephthaloyl chloride and *p*-phenylene diamine. The aromatic rings impart the rigid rodlike chain structure of aramid. These chains are highly oriented and extended along the fiber axis, with the resultant high modulus. Aramid fiber has a highly crystalline structure and the *para* orientation of the aromatic rings in the polymer chains results in a high packing efficiency. Strong covalent bonding in the fiber direction and weak hydrogen bonding in the transverse direction (see Fig. 2.34) result in highly anisotropic properties.

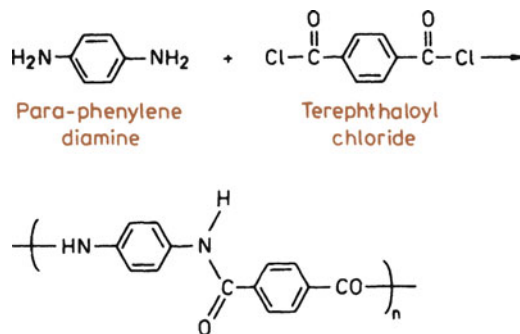
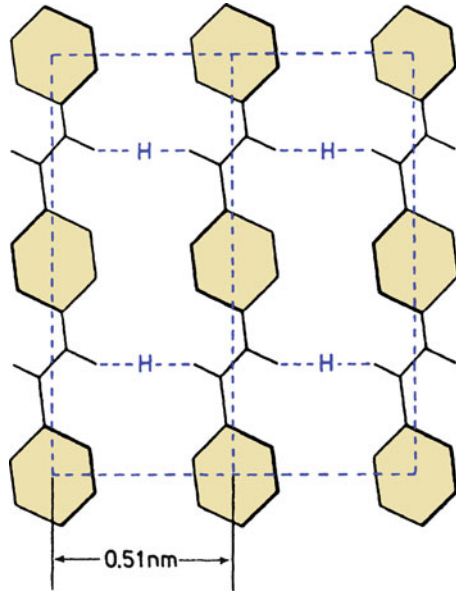


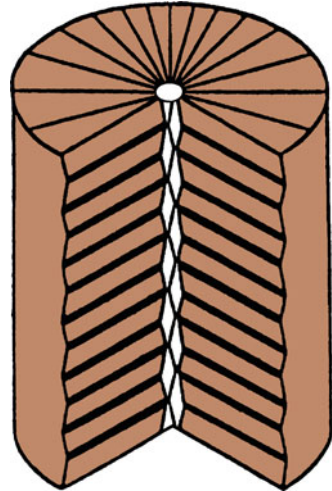
Fig. 2.33 Chemical structure of aramid fiber



**Fig. 2.34** Strong covalent bonding in the fiber direction and weak hydrogen bonding (indicated by *H*) in the transverse direction



**Fig. 2.35** Schematic representation of the supramolecular structure of aramid fiber, Kevlar 49. The structure consists of radially arranged, axially pleated crystalline sheets [from Dobb et al. (1980), used with permission]



The structure of Kevlar aramid fiber has been investigated by electron microscopy and diffraction. A schematic representation of the supramolecular structure of Kevlar 49 is shown in Fig. 2.35 (Dobb et al. 1980). It shows radially arranged, axially pleated crystalline supramolecular sheets. The molecules form a planar array with interchain hydrogen bonding. The stacked sheets form a crystalline

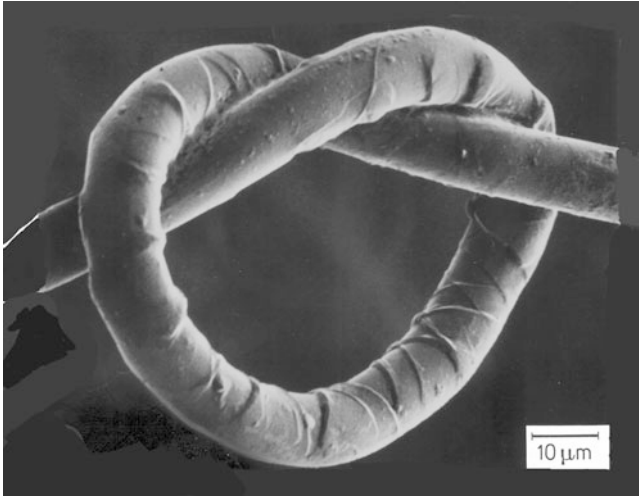


**Fig. 2.36** Knotted Kevlar aramid fiber showing buckling marks on the compressive side. The tensile side is smooth [courtesy of Fabric Research Corp.]

array, but between the sheets the bonding is rather weak. Each pleat is about 500 nm long, and the pleats are separated by transitional bands. The adjacent components of a pleat make an angle of  $170^\circ$ . Such a structure is consistent with the experimentally observed rather low-longitudinal shear modulus and poor properties in compression and transverse to the Kevlar fiber axis. A correlation between good compressive characteristics and a high glass transition temperature (or melting point) has been suggested (Northolt 1981). Thus, since the glass transition temperature of organic fibers is lower than that of inorganic fibers, the former would be expected to show poorer properties in compression. For aramid- and polyethylene-type high stiffness fibers, compression results in the formation of kink bands leading to an eventual ductile failure. Yielding is observed at about 0.5 % strain; this is thought to correspond to a molecular rotation of the amide carbon–nitrogen bond shown in Fig. 2.33 from the normal, extended, *trans* configuration to a kinked, *cis* configuration (Tanner et al. 1986). In the chemical literature, this is referred to as *cis–trans* isomerism. It describes the orientation of functional groups in a molecule. In aromatic structures, the rotation of bonds is greatly restricted. *Cis* in Latin means “on the same side” while *trans* means “on the other side” or “across.” This *trans* to *cis* rotation in the aramid fiber causes a  $45^\circ$  bend in the chain. This bend propagates across the unit cell, the microfibrils, and a kink band results in the fiber. This anisotropic behavior of aramid fiber is revealed in a vivid manner in the SEM micrograph of knotted fiber shown in Fig. 2.36. Note the buckling or kink marks on the compressive side of a knotted Kevlar aramid fiber. Note also the absence of such markings on the tensile side. Such markings on the aramid fiber surface have also been reported by, among others, DeTeresa et al. (1984) when the aramid fiber is subjected to uniform compression or torsion.

**Table 2.6** Properties of Kevlar aramid fiber yarns<sup>a</sup>

Property	K 29	K 49	K 119	K 129	K 149
Density (g/cm <sup>3</sup> )	1.44	1.45	1.44	1.45	1.47
Diameter (μm)	12	12	12	12	12
Tensile strength (GPa)	2.8	2.8	3.0	3.4	2.4
Tensile strain to fracture (%)	3.5–4.0	2.8	4.4	3.3	1.5–1.9
Tensile modulus (GPa)	65	125	55	100	147
Moisture regain (%) at 25 °C, 65 % RH	6	4.3	–	–	1.5
Coefficient of expansion (10 <sup>-6</sup> K <sup>-1</sup> )	-4.0	-4.9	–	–	–

<sup>a</sup>All data from Du Pont brochures. Indicative values only. 25-cm yarn length was used in tensile tests (ASTM D-885). *K* stands for Kevlar, a trademark of Du Pont

### 2.5.2.3 Properties and Applications of Aramid Fibers

Some of the important properties of Kevlar aramid fibers are summarized in Table 2.6. As can be seen from this table, the aramid fiber is very light and has very high stiffness and strength in tension. The two well-known varieties are Kevlar 49 and Kevlar 29. Kevlar 29 has about half the modulus but double the strain to failure of Kevlar 49. It is this high strain to failure of Kevlar 29 that makes it useful for making vests that are used for protection against small arms. It should be emphasized that aramid fiber, like most other high-performance organic fibers, has rather poor characteristics in compression, its compressive strength being only about 1/8 of its tensile strength. This follows from the anisotropic nature of the fiber as previously discussed. In tensile loading, the load is carried by the strong covalent bonds while in compressive loading, weak hydrogen bonding and van der Waals bonds come into play, which lead to rather easy local yielding, buckling, and kinking of the fiber. Thus, aramid-type high-performance fibers are not suitable for applications involving compressive forces.

Aramid fiber has good vibration-damping characteristics. Dynamic (commonly sinusoidal) perturbations are used to study the damping behavior of a material. The material is subjected to an oscillatory strain. We can characterize the damping behavior in terms of a quantity called the logarithmic decrement,  $\Delta$ , which is defined as the natural logarithm of the ratio of amplitudes of successive vibrations, i.e.,

$$\Delta = \ln \frac{\theta_n}{\theta_{n+1}},$$

where  $\theta_n$  and  $\theta_{n+1}$  are the two successive amplitudes. The logarithmic decrement is proportional to the ratio of maximum energy dissipated per cycle/maximum energy stored in the cycle. Composites of aramid fiber/epoxy matrix show a logarithmic decrement which is about five times that of glass fiber/epoxy.

Like other polymers, aramid fibers are sensitive to ultraviolet (UV) light. When exposed to ultraviolet light, aramid fibers discolor from yellow to brown and lose mechanical properties. Radiation of a particular wavelength can cause degradation

**Table 2.7** Properties of Technora fiber<sup>a</sup>

Density (g/cm <sup>3</sup> )	Diameter (μm)	Tensile strength (GPa)	Tensile modulus (GPa)	Tensile strain to fracture (%)
1.39	12	3.1	71	4.4

<sup>a</sup>Manufacturer's data; indicative values only

because of absorption by the polymer and breakage of chemical bonds. Near-UV and part of the visible spectrum should be avoided for outdoor applications involving use of unprotected aramid fibers. A small amount of such light emanates from incandescent and fluorescent lamps or sunlight filtered by window glass. Du Pont Co. recommends that Kevlar aramid yarn should not be stored within 1 ft (0.3 m) of fluorescent lamps or near windows.

The Technora fiber of Teijin shows properties that are a compromise between conventional fibers and rigid-rod fibers; Table 2.7 provides a summary of these. In terms of its stress–strain behavior, it can be said that Technora fiber lies between Kevlar 49 and Kevlar 29.

Different types of Kevlar aramid fibers provide an impressive set of properties, see Table 2.6. The three important types of Kevlar aramid fibers are used for specific applications (Magat 1980):

1. *Kevlar*. This is meant mainly for use as rubber reinforcement for tires (belts or radial tires for cars and carcasses of radial tires for trucks) and, in general, for mechanical rubber goods.
2. *Kevlar 29*. This is used for ropes, cables, coated fabrics for inflatables, architectural fabrics, and ballistic protection fabrics. Vests made of Kevlar 29 have been used by law-enforcement agencies in many countries.
3. *Kevlar 49*. This is meant for reinforcement of epoxy, polyester, and other resins for use in the aerospace, marine, automotive, and sports industries.

## 2.6 Ceramic Fibers

Continuous ceramic fibers present an attractive package of properties. They combine high strength and elastic modulus with high-temperature capability and a general freedom from environmental attack. These characteristics make them attractive as reinforcements in high-temperature structural materials.

There are three methods to fabricate ceramic fibers: chemical vapor deposition, polymer pyrolysis, and sol–gel techniques. The latter two involve rather novel techniques of obtaining ceramics from organometallic polymers. The sol–gel technique was mentioned in Sect. 2.2 in regard to the manufacture of silica-based glass fibers. The sol–gel technique is also used to produce a variety of alumina-based oxide fibers commercially. Another breakthrough in the ceramic fiber area is the concept of pyrolyzing; under controlled conditions, polymers containing silicon

and carbon or nitrogen can be converted to high-temperature ceramic fibers. This idea is nothing but an extension of the polymer pyrolysis route to produce a variety of carbon fibers wherein a suitable carbon-based polymer (e.g., PAN or pitch) is subjected to controlled heating to produce carbon fibers (see Sect. 2.4). The pyrolysis route of producing ceramic fibers has been used with polymers containing silicon, carbon, nitrogen, and boron, with the end products being SiC, Si<sub>3</sub>N<sub>4</sub>, B<sub>4</sub>C, and BN in fiber form, foam, or coating. We describe some important ceramic fibers.

### 2.6.1 Oxide Fibers

Many alumina-type oxide fibers are available commercially. Alumina has many allotropic forms:  $\gamma$ ,  $\delta$ ,  $\eta$ , and  $\alpha$ . Of these,  $\alpha$ -alumina is the most stable form. A variety of alumina-based continuous fibers made by sol-gel processing are available commercially. The sol-gel process of making fibers involves the following steps, common to all fibers:

1. Formulate sol.
2. Concentrate to form a viscous gel.
3. Spin the precursor fiber.
4. Calcine to obtain the oxide fiber.

3M Co. produces a series of ceramic fibers called the Nextel fibers. They are mainly Al<sub>2</sub>O<sub>3</sub> + SiO<sub>2</sub> and some B<sub>2</sub>O<sub>3</sub>. The composition and properties of some Nextel fibers are given in Table 2.8. Figure 2.37 shows an optical micrograph of Nextel 312 fibers. The sol-gel manufacturing process used by 3M Co. has metal

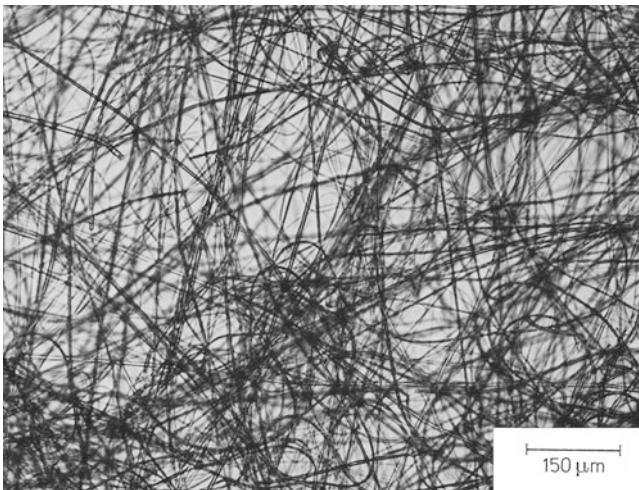


**Fig. 2.37** Optical micrograph of Nextel 312 (Al<sub>2</sub>O<sub>3</sub> + B<sub>2</sub>O<sub>3</sub> + SiO<sub>2</sub>) fiber

**Table 2.8** Composition and properties of some oxide fibers<sup>a</sup>

Fiber type	Composition (wt.%)	Diameter ( $\mu\text{m}$ )	Density, ( $\text{g}/\text{cm}^3$ )	Tensile strength (GPa)	Young's modulus (GPa)
Nextel 312	$\text{Al}_2\text{O}_3$ -62.5, $\text{SiO}_2$ -24.5, $\text{B}_2\text{O}_3$ -13	10–12	2.70	1.7	150
Nextel 440	$\text{Al}_2\text{O}_3$ -70, $\text{SiO}_2$ -28, $\text{B}_2\text{O}_3$ -2	10–12	3.05	2.0	190
Nextel 550	$\text{Al}_2\text{O}_3$ -73, $\text{SiO}_2$ -27	10–12	3.03	2.0	193
Nextel 610	$\text{Al}_2\text{O}_3$ -99+	10–12	3.9	3.1	370
Nextel 650	$\text{Al}_2\text{O}_3$ -89, $\text{ZrO}_2$ -10, $\text{Y}_2\text{O}_3$ -1	10–12	4.10	2.5	358
Nextel 720	$\text{Al}_2\text{O}_3$ -85, $\text{SiO}_2$ -15	10–12	3.40	2.1	260
Saffil	$\text{Al}_2\text{O}_3$ -96, $\text{SiO}_2$ -4	3	2.3	1.0	100
Saphikon	Single Crystal $\text{Al}_2\text{O}_3$	75–250	3.8	3.1	380
Sumitomo	$\text{Al}_2\text{O}_3$ -85, $\text{SiO}_2$ -15	9	3.2	2.6	250

<sup>a</sup>Manufacturer's data

alkoxides as the starting materials. The reader will recall that metal alkoxides are  $M(OR)_n$ -type compounds, where  $M$  is the metal,  $n$  is the metal valence, and  $R$  is an organic compound. Selection of an appropriate organic group is very important. It should provide sufficient stability and volatility to the alkoxide so that  $M-OR$  bonds are broken and  $MO-R$  is obtained to give the desired oxide ceramics. Hydrolysis of metal alkoxides results in sols that are spun and gelled. The gelled fiber is then densified at relatively low temperatures. The high surface free energy available in the pores of the gelled fiber allows for densification at relatively low temperatures. The sol–gel process provides close control over solution composition and rheology of fiber diameter. The disadvantage is that rather large dimensional changes must be accommodated and fiber integrity preserved.

Sowman (1988) has provided details of the process used by 3M Co. for making the Nextel oxide fibers. Aluminum acetate [ $\text{Al}(\text{OH})_2(\text{OOCCH}_3) \cdot 1/3\text{H}_3\text{BO}_3$ ], e.g., “Niaproof,” from Niacet Corp., is the starting material. Aluminum acetate with an  $\text{Al}_2\text{O}_3/\text{B}_2\text{O}_3$  ratio of 3 to 1 becomes spinnable after water removal from an aqueous solution. In the fabrication of 3M continuous fibers, a 37.5 % solution of basic aluminum acetate in water is concentrated in a rotating flask partially immersed in a water bath at 32–36 °C. After concentration to an equivalent  $\text{Al}_2\text{O}_3$  content of 28.5 %, a viscous solution with viscosity,  $\eta$ , between 100 and 150 Pa s is obtained. This is extruded through a spinneret under a pressure of 800–1,000 kPa. Shiny, colorless fibers are obtained on firing to 1,000 °C. The microstructure shows cube- and lath-shaped crystals. The boria addition lowers the temperature required for mullite formation and retards the transformation of alumina to  $\alpha$ - $\text{Al}_2\text{O}_3$ . One needs boria in an amount equivalent to or greater than a 9  $\text{Al}_2\text{O}_3$ :2  $\text{B}_2\text{O}_3$  ratio in  $\text{Al}_2\text{O}_3$ – $\text{B}_2\text{O}_3$ – $\text{SiO}_2$  compositions to prevent the formation of crystalline alumina.

Crystalline alumina fibers are also made via sol–gel. Boric salts of aluminum decompose into transition aluminum oxide spinels such as  $\eta$ - $\text{Al}_2\text{O}_3$  above 400 °C.

These transition cubic spinels convert to hexagonal  $\alpha$ - $\text{Al}_2\text{O}_3$  on heating to between 1,000 and 1,200 °C. The problem is that the nucleation rate of pure  $\alpha$ - $\text{Al}_2\text{O}_3$  is too low and results in rather large grains. Also, during the transformation to  $\alpha$  phase, a large shrinkage results in a rather large porosity. The  $\alpha$ - $\text{Al}_2\text{O}_3$  fiber, 3 M Co.'s tradename Nextel 610, is obtained by seeding the high-temperature  $\alpha$ -alumina with a very fine hydrous colloidal iron oxide. The fine iron oxide improves the nucleation rate of  $\alpha$ - $\text{Al}_2\text{O}_3$ , resulting in a high-density, ultrafine, homogeneous  $\alpha$ - $\text{Al}_2\text{O}_3$  fiber (Wilson 1990).  $\alpha$ - $\text{Fe}_2\text{O}_3$  is isostructural with  $\alpha$ - $\text{Al}_2\text{O}_3$  (5.5 % lattice mismatch). 3M's hydrous colloidal iron oxide sol appears to be an efficient nucleating agent. Without the seeding with iron oxide, the  $\eta$ -alumina-to- $\alpha$ -alumina transformation occurred at about 1,100 °C. With 1 %  $\text{Fe}_2\text{O}_3$ , the transformation temperature was decreased to 1,010 °C, while with 4 %  $\text{Fe}_2\text{O}_3$ , the transformation temperature came down to 977 °C. Concomitantly, the grain size was refined. In addition to  $\text{Fe}_2\text{O}_3$ , about 0.5 wt.%  $\text{SiO}_2$  is added to reduce the final grain size of Nextel 610 fiber, although  $\text{SiO}_2$  inhibits the transformation to the  $\alpha$  phase. The  $\text{SiO}_2$  addition also reduces grain growth during soaking at 1,400 °C.

Many other alumina- or alumina-silica-type fibers are available. Most of these are also made by the sol-gel process. Sumitomo Chemical Co. produces a fiber that is a mixture of alumina and silica. The flow diagram of this process is shown in Fig. 2.38. Starting from an organoaluminum (polyaluminumoxanes or a mixture of polyaluminumoxanes and one or more kinds of Si-containing compounds), a precursor fiber is obtained by dry spinning. This precursor fiber is calcined to produce the final fiber. The fiber structure consists of fine crystallites of spinel.  $\text{SiO}_2$  serves to stabilize the spinel structure and prevents it from transforming to  $\alpha$ - $\text{Al}_2\text{O}_3$ . Yet another variety of alumina fiber available commercially is a  $\delta$ - $\text{Al}_2\text{O}_3$ , a staple fiber (tradename *Saffil*). This fiber has about 4 %  $\text{SiO}_2$  and a very fine diameter (3  $\mu\text{m}$ ). The starting material for Saffil is an aqueous phase containing an oxide sol and an organic polymer: Aluminum oxychloride [ $\text{Al}_2(\text{OH})_5\text{Cl}$ ] is mixed with a medium-molecular-weight polymer such as 2 wt.% polyvinyl alcohol. The sol is extruded as filaments into a coagulating (or precipitating) bath in which the extruded shape gels. The gelled fiber is then dried and calcined to produce the final oxide fiber. This solution is slowly evaporated in a rotary evaporator until a viscosity of about 80 Pa s (800 P) is attained. This solution is extruded through a spinneret, the fibers are wound on a drum, and fired to about 800 °C. The organic material is burned away, and a fine-grain alumina fiber with 5–10 % porosity and a diameter of 3–5  $\mu\text{m}$  is obtained. The fibers as produced at this stage are suitable for filtering purposes because of their high porosity. By heating them to 1,400–1,500 °C, which causes 3–4 % of linear shrinkage, one obtains a refractory alumina fiber suitable for reinforcement purposes. Care is taken to produce fibers with diameter greater than 1  $\mu\text{m}$  (to avoid biological hazards) but less than 6  $\mu\text{m}$  (to avoid skin irritation).

A technique called *edge-defined film-fed growth* (EFG) has been used to make continuous, monocrystalline sapphire ( $\text{Al}_2\text{O}_3$ ) fiber (LaBelle and Mlavsky 1967; LaBelle 1971; Pollack 1972; Hurley and Pollack 1972). LaBelle and Mlavsky (1967) grew sapphire ( $\text{Al}_2\text{O}_3$ ) single-crystal fibers using a modified Czochralski puller and radio frequency heating. The process is called the edge-defined film-fed

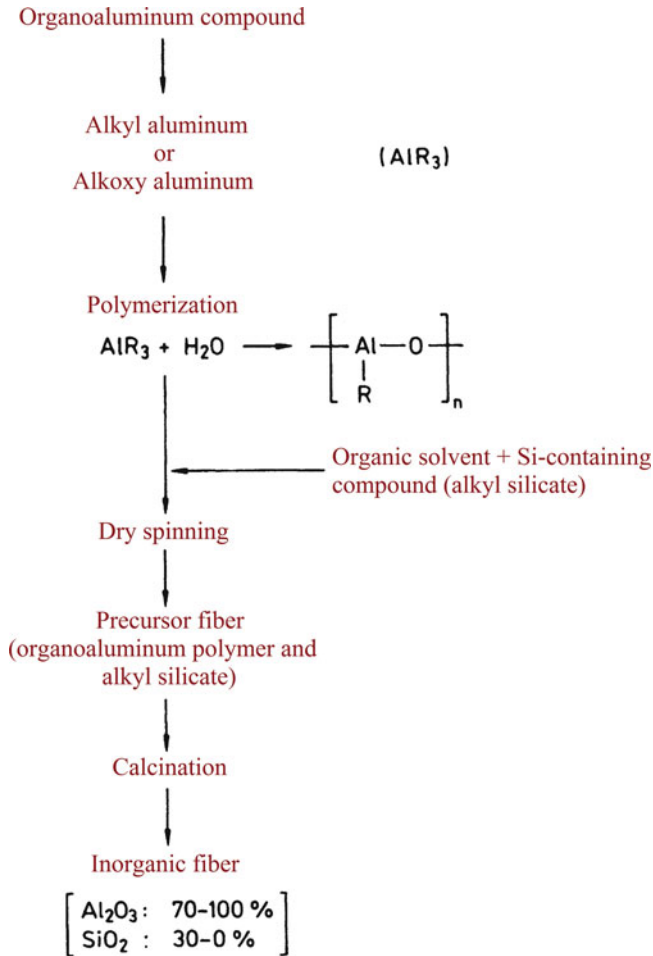


Fig. 2.38 Flow diagram of an alumina + silica fiber production

growth method because the external edge of the die defines the shape of the fiber and the liquid is fed in the form of a film. Fiber growth rates as high as 200 mm/min have been attained. The die material must be stable at the melting point of alumina; a molybdenum die is commonly used. A capillary supplies a constant liquid level at the crystal interface. A sapphire seed crystal is used to control the orientation of the single crystal fiber. Molten alumina wets both molybdenum and alumina. The crystal grows from a molten film between the growing crystal and the die. The crystal shape is defined by the external shape of the die rather than the internal shape. A commercial fiber produced by this method, called *Saphikon*, has a hexagonal structure with its *c*-axis parallel to the fiber axis. The diameter (actually it has rounded triangular cross-section) is rather large, between 125 and 250  $\mu\text{m}$ .



A *laser-heated floating zone method* has been devised to make a variety of ceramic fibers. Gasson and Cockayne (1970) used laser heating for crystal growth of  $\text{Al}_2\text{O}_3$ ,  $\text{Y}_2\text{O}_3$ ,  $\text{MgAl}_2\text{O}_4$ , and  $\text{Na}_2\text{O}_3$ . Haggerty (1972) used a four-beam laser-heated float zone method to grow single-crystal fibers of  $\text{Al}_2\text{O}_3$ ,  $\text{Y}_2\text{O}_3$ ,  $\text{TiC}$ , and  $\text{TiB}_2$ . A  $\text{CO}_2$  laser is focused on the molten zone. A source rod is brought into the focused laser beam. A seed crystal, dipped into the molten zone, is used to control the orientation. Crystal growth starts by moving the source and seed rods simultaneously. Mass conservation dictates that the diameter be reduced as the square root of the feed rate/pull rate ratio. It is easy to see that, in this process, the fiber purity is determined by the purity of the starting material.

### 2.6.2 Nonoxide Fibers

Nonoxides such as silicon carbide and silicon nitride have very attractive properties. Silicon carbide, in particular, is commercially available in a fibrous form. In this section, we describe some of these nonoxide fibers.

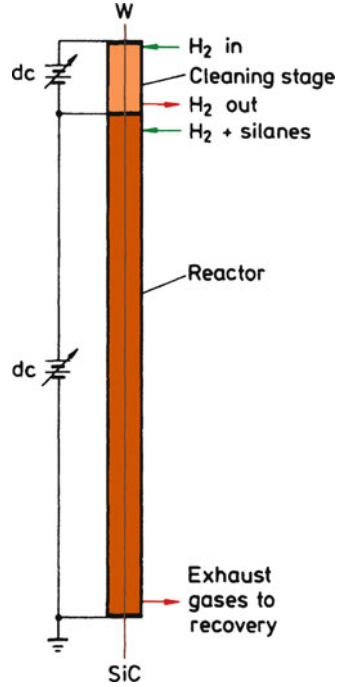
#### 2.6.2.1 Silicon Carbide Fibers by CVD

Silicon carbide fiber must be regarded as a major development in the field of ceramic reinforcements during the last quarter of the twentieth century. In particular, a process developed by the late Professor Yajima in Japan, involving controlled pyrolysis of a polycarbosilane (PCS) precursor to yield a small diameter, flexible fiber, must be considered to be the harbinger of the manufacture of ceramic fibers from polymeric precursors. In this section, we describe the processing, microstructure, and properties of the silicon carbide fibers in some detail.

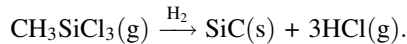
We can easily classify the fabrication methods for SiC as conventional or nonconventional. The conventional category would include CVD while the nonconventional would include controlled pyrolysis of polymeric precursors. There is yet another important type of SiC available for reinforcement purposes: SiC whiskers.

Silicon carbide fiber can be made by CVD on a substrate heated to approximately 1,300 °C. The substrate can be tungsten or carbon. The reactive gaseous mixture contains hydrogen and alkyl silanes. Typically, a gaseous mixture consisting of 70 % hydrogen and 30 % silanes is introduced at the reactor top (Fig. 2.39), where the tungsten substrate (~13  $\mu\text{m}$  diameter) also enters the reactor. Mercury seals are used at both ends as contact electrodes for the filament. The substrate is heated by combined direct current (250 mA) and very high frequency (VHF ~60 MHz) to obtain an optimum temperature profile. To obtain a 100- $\mu\text{m}$  SiC monofilament, it generally takes about 20 s in the reactor. The filament is wound on a spool at the bottom of the reactor. The exhaust gases (95 % of the original mixture + HCl) are passed around a condenser to recover the unused silanes.

**Fig. 2.39** CVD process for SiC monofilament fabrication [From J.V. Milewski et al. (1974), reproduced with permission]



Efficient reclamation of the unused silanes is very important for a cost-effective production process. This CVD process of making SiC fiber is very similar to that of B fiber manufacture. The nodules on the surface of SiC are smaller than those seen on B fibers. Such CVD processes result in composite monofilaments that have built-in residual stresses. The process is, of course, very expensive. Methyltrichlorosilane is an ideal raw material, as it contains one silicon and one carbon atom, i.e., one would expect a stoichiometric SiC to be deposited. The chemical reaction is:



An optimum amount of hydrogen is required. If the hydrogen is less than sufficient, chlorosilanes will not be reduced to Si and free carbon will be present in the mixture. If too much hydrogen is present, the excess Si will form in the end product. Generally, solid (free) carbon and solid or liquid silicon are mixed with SiC. The final monofilament (100–150  $\mu\text{m}$ ) consists of a sheath of mainly  $\beta$ -SiC with some  $\alpha$ -SiC on the tungsten core. The {111} planes in SiC deposit are parallel to the fiber axis. The cross-section of SiC monofilament resembles closely that of a boron fiber. Properties of a CVD SiC monofilament are given in Table 2.9.

Commercially, a series of surface-modified silicon carbide fibers, called SCS fibers is available. These special fibers have a complex through the thickness gradient structure. SCS-6, for example, is a thick fiber (diameter = 142  $\mu\text{m}$ ) that is produced by CVD of silicon- and carbon-containing compounds onto a pyrolytic graphite-coated carbon fiber core. The pyrolytic graphite coating is applied to a carbon monofilament to give a substrate of 37  $\mu\text{m}$ . This is then coated with SiC by CVD to give a final monofilament of 142  $\mu\text{m}$  diameter. Figure 2.40 shows schematically the SCS-6 silicon carbide fiber and its characteristic surface compositional gradient. The surface modification of the SCS-6 fibers consists of the following. The bulk of the 1- $\mu\text{m}$ -thick surface coating consists of C-doped Si. Zone I at and near the surface is a carbon-rich zone. In zone II, Si content decreases. This is followed by zone III in which the Si content increases back to the stoichiometric SiC composition. Thus, the SCS-6 silicon carbide fiber has a carbon rich surface and back to stoichiometric SiC a few micrometer from the surface.

Another CVD-type silicon carbide fiber is called *sigma fiber*. Sigma fiber is a continuous silicon carbide monofilament by CVD on a tungsten substrate.

**Table 2.9** Properties of CVD SiC monofilament

Composition	Diameter ( $\mu\text{m}$ )	Density ( $\text{g}/\text{cm}^3$ )	Tensile strength (MPa)	Young's modulus (GPa)
$\beta$ -SiC	140	3.3	3,500	430

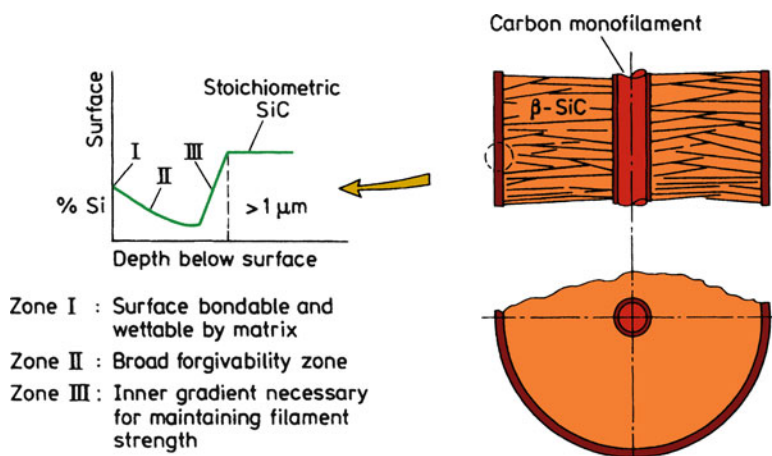


**Fig. 2.40** Schematic of SCS-6 silicon carbide fiber and its surface compositional gradient (courtesy of Textron Specialty Materials Co.)

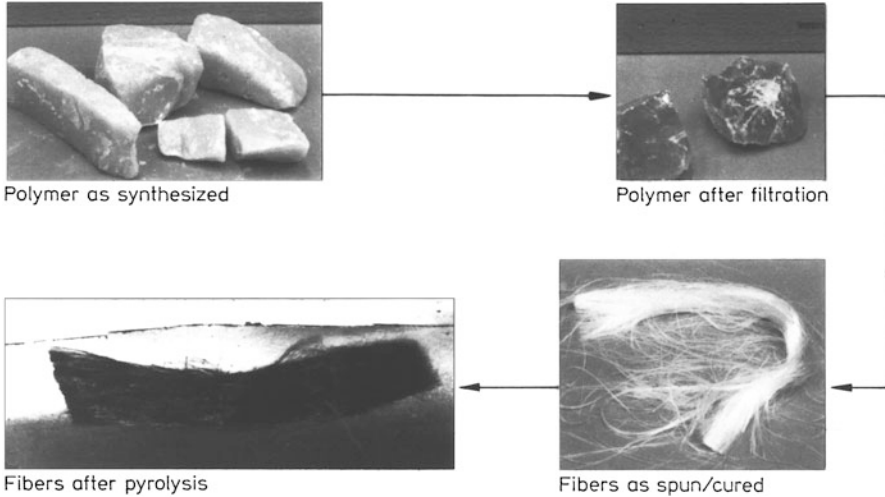


**Fig. 2.41** Schematic of ceramic fiber production starting from silicon-based polymers [adapted from Wax (1985), used with permission]

### 2.6.2.2 Nonoxide Fibers via Polymers

As pointed out earlier, the SiC fiber obtained via CVD is very thick and not very flexible. Work on alternate routes of obtaining fine, continuous, and flexible fiber had been ongoing, when in the mid-1970s the late Professor Yajima and his colleagues (1976, 1980) in Japan developed a process of making such a fiber by controlled pyrolysis of a polymeric precursor. This method of using silicon-based polymers to produce a family of ceramic fibers with good mechanical properties, good thermal stability, and oxidation resistance has enormous potential. The various steps involved in this polymer route, shown in Fig. 2.41 (Wax 1985), are:

1. Synthesis and characterization of polymer (yield, molecular weight, purity, and so on).
2. Melt spin polymer into a precursor fiber.
3. Cure the precursor fiber to cross-link the molecular chains, making it infusible during the final stage of pyrolysis.

Specifically, the Yajima process of making SiC involves the following steps and is shown schematically in Fig. 2.42. PCS, a high-molecular-weight polymer containing Si and C, is synthesized. The starting material is commercially available dimethylchlorosilane. Solid polydimethylsilane (PDMS) is obtained by dechlorination of dimethylchlorosilane by reacting it with sodium. PCS is obtained by thermal decomposition and polymerization of PDMS. This is carried out under high pressure in an autoclave at 470 °C in an argon atmosphere for 8–14 h. A vacuum distillation treatment at up to 280 °C follows. The average molecular weight of the resulting polymer is about 1,500. This is melt spun from a 500-hole spinneret at

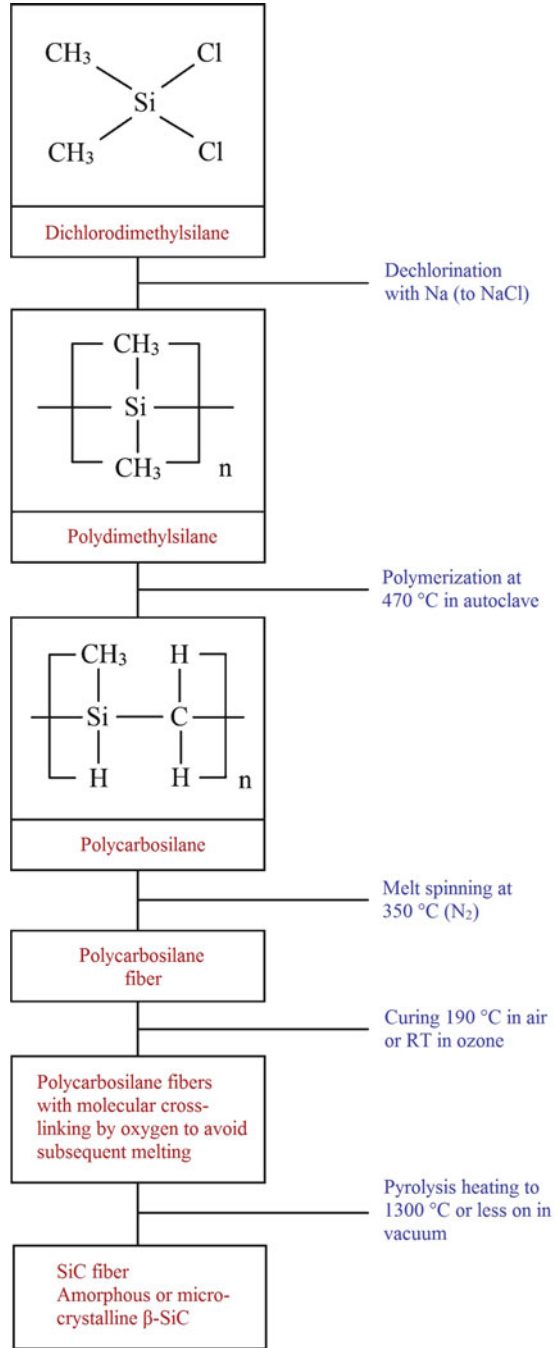
about 350 °C in nitrogenous atmosphere to obtain the preceramic continuous, precursor fiber. The precursor fiber is quite weak (tensile strength ~ 10 MPa). This is converted to inorganic SiC by curing in air, heating to about 1,000 °C in N<sub>2</sub> gas, followed by heating to 1,300 °C in N<sub>2</sub> under stretch. This is basically the Nippon Carbon Co. manufacture process for Nicalon (the commercial name of fine diameter silicon carbide fiber) fibers (Andersson and Warren 1984; Simon and Bunsell 1984). During the pyrolysis, the first stage of conversion occurs at approximately 550 °C when cross-linking of polymer chains occurs. Above this temperature, the side chains containing hydrogen and methyl groups decompose. Fiber density and mechanical properties improve sharply. The conversion to SiC takes place above about 850 °C.

There are different grades of Nicalon (nominally SiC) available commercially. The properties of the first generation of Nicalon fiber were less than desirable, they would start degrading above about 600 °C because of the thermodynamic instability of composition and microstructure. A ceramic-grade Nicalon fiber, called NLP-202, having low oxygen content is also available and shows better high-temperature properties. Yet another version of multifilament silicon carbide fiber is Tyranno. This is made by pyrolysis of poly (titano carbosilane), and it contains between 1.5 and 4 wt.% titanium.

Fine-diameter, polymer-derived silicon carbide fibers, such as Nicalon, generally have high oxygen content. This results from the curing of the precursor fibers in an oxidizing atmosphere to introduce cross-linking. Cross-linking is required to make the precursor fiber infusible during the subsequent pyrolysis step. One way around this is to use electron beam curing. Other techniques involve dry spinning of high-molecular-weight PCS polymers (Sacks et al. 1995). In this case, the as-spun fiber does not require a curing step because of the high-molecular-weight PCS polymer used, i.e., it does not melt during pyrolysis without requiring curing. Sacks et al. (1995) used dopants to produce low-oxygen, near-stoichiometric, small-diameter (10–15 μm) SiC fibers. They reported an average tensile strength for these fibers of about 2.8 GPa. Their fiber had a C-rich and near stoichiometric SiC and low oxygen content (Sacks et al. 1995; Toreki et al. 1994). They started with PDMS, which has an Si–Si backbone. This is subjected to pressure pyrolysis to obtain PCS, which has an Si–C backbone. The key point in their process is to have a molecular weight of PCS between 5,000 and 20,000. This is a high molecular weight compared to that used in other processes. The spinning dope was obtained by adding suitable spinning aids and a solvent. This dope was dry spun to produce *green fibers*, which were heated under controlled conditions to produce SiC fiber.

Laine and coworkers (1993, 1995) and Zhang et al. (1994) have used a polymethylsilane (PMS) ([CH<sub>3</sub>SiH]<sub>x</sub>) as the precursor polymer for making a fine-diameter, silicon carbide fiber. Spinning aids were used to stabilize the polymer solution and the precursor fiber was extruded from a 140-μm orifice extruder into an argon atmosphere. The precursor fiber was pyrolyzed at 1,800 °C in Ar. Boron, added as a sintering aid, helped to obtain a dense product.

**Fig. 2.42** Schematic of SiC (Nicalon) production [adapted from Andersson and Warren (1984), used with permission]



Another silicon carbide multifilament fiber made via a polymeric precursor and available commercially is called *Sylramic*. According to the manufacturer, this textile-grade silicon carbide fiber is a nanocrystalline, stoichiometric silicon carbide (crystallite size of 0.5  $\mu\text{m}$ ). Its density is 3.0  $\text{g}/\text{cm}^3$ , and it has average tensile strength and modulus of 3.15 and 405 GPa, respectively.

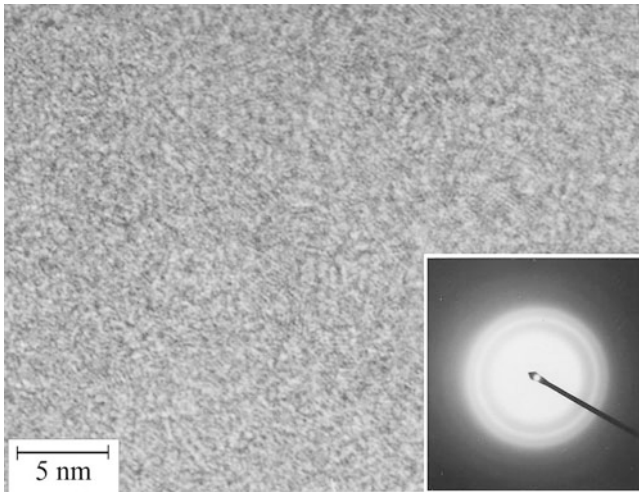


**Fig. 2.43** High-resolution transmission electron micrograph of Nicalon fiber showing its amorphous structure [courtesy of K. Okamura]

### 2.6.2.3 Structure and Properties

The structure of Nicalon fiber has been studied by a number of researchers. Figure 2.43 shows a high-resolution transmission electron micrograph of Nicalon-type SiC produced in laboratory, indicating the amorphous nature of the SiC produced by the Yajima process. The commercial variety of Nicalon has an amorphous structure while another, noncommercial variety, showed a microcrystalline structure (SiC grain radius of 1.7 nm) (Laffon et al. 1989). The microstructural analysis shows that both fibers contain  $\text{SiO}_2$  and free carbon in addition to SiC. The density of the fiber is about 2.6  $\text{g}/\text{cm}^3$ , which is low compared to that of pure  $\beta$ -SiC, which is not surprising because the composition of Nicalon fiber is a mixture of SiC,  $\text{SiO}_2$ , and C.

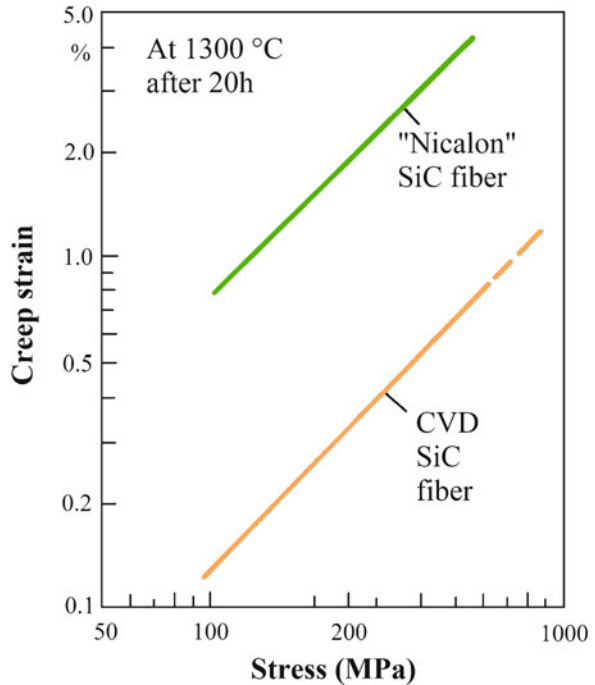
The properties of various fine diameter, polymer-derived SiC type fibers are summarized in Table 2.10. One would expect CVD SiC fiber to show superior creep properties vis à vis Nicalon fiber, mainly because CVD SiC fiber has mostly  $\beta$ -SiC while the Nicalon fiber is a mixture of SiC,  $\text{SiO}_2$ , and free carbon. This is shown in Fig. 2.44 where we show a log–log plot of creep strain as a function of stress for Nicalon and CVD SiC fiber. Notice the superior performance of the CVD SiC fiber. Recall that the CVD SiC fiber has a large diameter, and thus is not flexible.

**Table 2.10** Properties of some fine-diameter SiC type fibers<sup>a</sup>

Fiber	Tensile strength (GPa)	Young's modulus (GPa)	Coefficient of thermal expansion ( $10^{-6} \text{ K}^{-1}$ )
Nicalon 200	2	200	3.2
Hi-Nicalon	2.8	270	3.5
Hi-Nicalon S	2.5	400	–
Sylramic iBN	3.5	400	5.4
Tyranno SA3	2.9	375	–

<sup>a</sup>After A. R. Bunsell and A. Piant (2006)

**Fig. 2.44** Comparison of creep strain in CVD SiC and Nicalon fibers (reprinted with permission from J Metals 37, No. 6, 1985, a publication of the Metallurgical Society, Warrendale PA)



## 2.7 Whiskers

*Whiskers* are monocrystalline, short fibers with extremely high strength. This high strength, approaching the theoretical strength, comes about because of the absence of crystalline imperfections such as dislocations. Being monocrystalline, there are no grain boundaries either. Typically, whiskers have a diameter of a few micrometers and a length of a few millimeters. Thus, their aspect ratio (length/diameter) can vary from 50 to 10,000. Whiskers do not have uniform dimensions or properties. This is perhaps their greatest disadvantage, i.e., the spread in properties is extremely large. Handling and alignment of whiskers in a matrix to produce a composite are other problems.



Whiskers are normally obtained by vapor phase growth. Back in the 1970s, a new process was developed that used rice hulls as the starting material to produce SiC particles and whiskers (Lee and Cutler 1975; Milewski et al. 1974). The SiC particles produced by this process are of a fine size. Rice hulls are a waste by-product of rice milling. For each 100 kg of rice milled, about 20 kg of rice hull is produced. Rice hulls contain cellulose, silica, and other organic and inorganic materials. Silica from soil is dissolved and transported in the plant as monosilicic acid. This is deposited in the cellulosic structure by liquid evaporation. It turns out that most of the silica ends up in hull. It is the intimate mixture of silica within the cellulose that gives the near-ideal amounts of silica and carbon for silicon carbide production. Raw rice hulls are heated in the absence of oxygen at about 700 °C to drive out the volatile compounds. This process is called *coking*. Coked rice hulls, containing about equal amounts of SiO<sub>2</sub> and free C, are heated in inert or reducing atmosphere (flowing N<sub>2</sub> or NH<sub>3</sub> gas) at a temperature between 1,500 and 1,600 °C for about 1 h to form silicon carbide as per the following reaction:

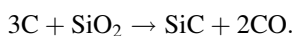
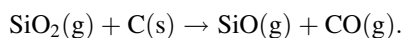
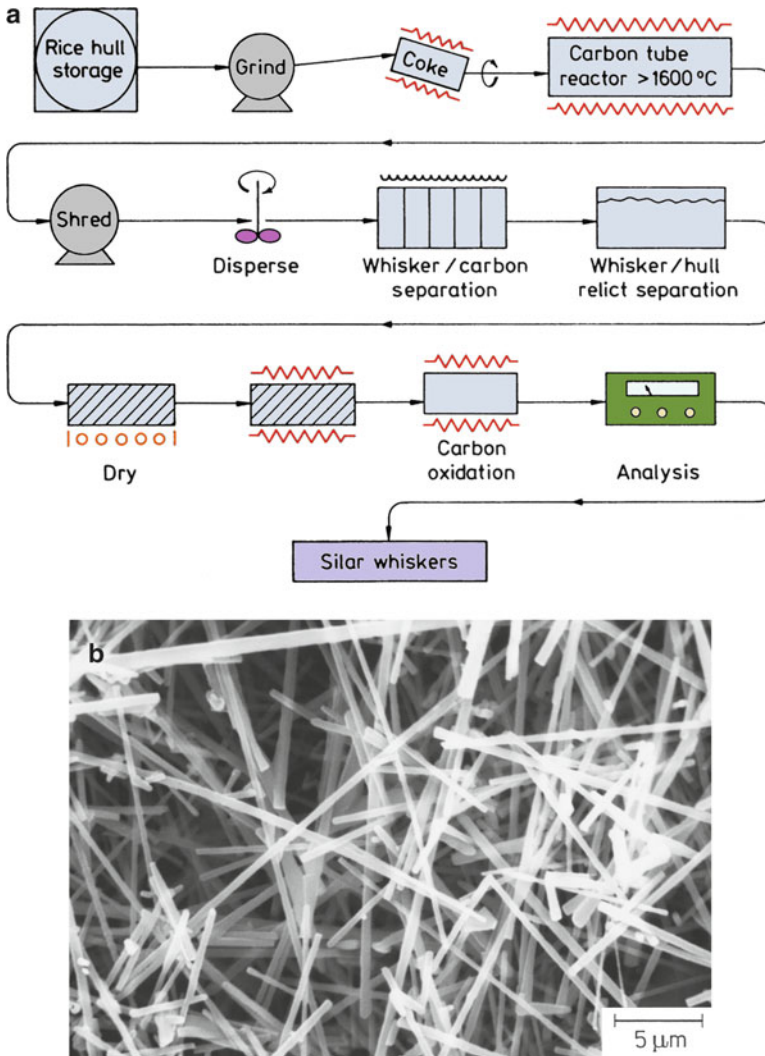


Figure 2.45 shows the schematic of the process. When the reaction is over, the residue is heated to 800 °C to remove any free C. Generally, both particles and whiskers are produced, together with some excess free carbon. A wet process is used to separate the particles and the whiskers. Typically, the average aspect ratio of the as-produced whiskers is 75.

Exceptionally strong and stiff silicon carbide whiskers have been grown using the so-called VLS process (Milewski et al. 1985; Petrovic et al. 1985). The average tensile strength and modulus were 8.4 and 581 GPa, respectively. The acronym VLS stands for *vapor* feed gases, *liquid* catalyst, and *solid* crystalline whiskers. In this process, the catalyst forms a liquid solution interface with the growing crystalline phase, while elements are fed from the vapor phase through the liquid–vapor interface. Whisker growth takes place by precipitation from the supersaturated liquid at the solid–liquid interface. The catalyst must take in solution the atomic species of the whisker to be grown. For SiC whiskers, transition metals and iron alloys meet this requirement. Figure 2.46 illustrates the process for SiC whisker growth. Steel particles (~30 μm) are used as the catalyst. At 1,400 °C, the solid steel catalyst particle melts and forms a liquid catalyst ball. From the vapor feed of SiC, H<sub>2</sub>, and CH<sub>4</sub>, the liquid catalyst extracts C and Si atoms and forms a supersaturated solution. The gaseous silicon monoxide is generated as per the following reaction:



The supersaturated solution of C and Si in the liquid catalyst precipitates out solid SiC whisker on the substrate. As the precipitation continues, the whisker grows (Fig. 2.46). Generally, the process results in a range of whisker morphologies. The tensile strength values vary a lot, they ranged from 1.7 to 23.7 GPa in 40 tests. Whisker lengths were about 10 mm; the equivalent circular diameter averaged 5.9 μm.



**Fig. 2.45** (a) Schematic of SiC whisker production process starting from rice hulls. (b) Scanning electron micrograph of SiC whiskers obtained from rice hulls [courtesy of Advanced Composite Materials Corporation (formerly Arco)]

## 2.8 Other Nonoxide Reinforcements

In addition to silicon carbide-based ceramic fibers, there are other promising ceramic fibers, e.g., silicon nitride, boron carbide, and boron nitride.

Silicon nitride ( $\text{Si}_3\text{N}_4$ ) fibers can be prepared by reactive CVD using volatile silicon compounds. The reactants are generally  $\text{SiCl}_4$  and  $\text{NH}_3$ .  $\text{Si}_3\text{N}_4$  is deposited

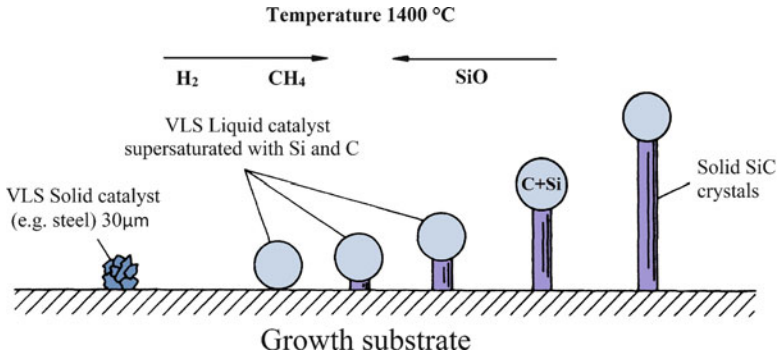


**Fig. 2.46** The VLS process for SiC whisker growth [after Milewski et al. (1985), used with permission]

on a carbon or tungsten substrate. Again, as in other CVD processes, the resultant fiber has good properties, but the diameter is very large and it is expensive. In the polymer route, organosilazane polymers with methyl groups on Si and N have been used as silicon nitride precursors. Such carbon-containing, silicon–nitrogen precursors, on pyrolysis, give silicon carbide as well as silicon nitride, i.e., the resulting fiber is not an SiC-free silicon nitride fiber. Wills et al. (1983) have discussed the mechanisms involved in the conversion of various organometallic compounds into ceramics.

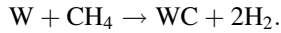
### 2.8.1 Silicon Carbide in a Particulate Form

SiC in particulate form has been available quite cheaply and abundantly for abrasive, refractories, and chemical uses. In this conventional process, silica in the form of sand and carbon in the form of coke are made to react at 2,400 °C in an electric furnace. The SiC produced in the form of large granules is subsequently comminuted to the desired size.

### 2.8.2 Tungsten Carbide Particles

Tungsten carbide is made by carburization of tungsten metal, which in turn, is prepared by hydrogen reduction of tungsten oxide. A mixture of tungsten powder and carbon black in the appropriate particle size and distribution is obtained by ball milling. The addition of carbon black helps control particle size and size distribution. The objective is to produce stoichiometric tungsten carbide with a small excess of free carbon, which prevents the formation of the highly undesirable *eta*-phase. Carburization is done in the presence of hydrogen at temperatures between

1,400 and 2,650 °C. The hydrogen reacts with the carbon black to form gaseous hydrocarbons, which react with tungsten to form tungsten carbide per the following reaction:



Commonly, after carburization, WC particles are deagglomerated by milling. The final particle size can range from 0.5 to 30  $\mu\text{m}$ . The particles are generally quite angular.

## 2.9 Effect of High-Temperature Exposure on the Strength of Ceramic Fibers

Carbon fiber is excellent at high temperatures in an inert atmosphere. In air, at temperatures above 400–450 °C, it starts oxidizing. SiC and  $\text{Si}_x\text{N}_y$  show reasonable oxidation resistance for controlled composition fibers. SiC starts oxidizing above 1,300–1,400 °C in air. The high-temperature strength of the SiC-type fibers is limited by oxidation and internal void formation, while in the case of oxide fibers any intergranular glassy phase leads to softening. Mah et al. (1984) studied the degradation of Nicalon fiber after heat treatment in different environments. The strength degradation of this fiber at temperatures greater than 1,200 °C was because of CO evaporation from the fiber as well as  $\beta$ -SiC grain growth. Ceramic fibers made via pyrolysis of polymeric precursors, especially with compositions Si–C–O and Si–N–C–O, have lower densities than the theoretical values (Lipowitz et al. 1990). The theoretical density,  $\rho_t$ , can be calculated using the relationship

$$\rho_t = \rho_i V_i,$$

where  $\rho$  is the density,  $V$  is the volume fraction, the subscript  $i$  indicates the  $i$ th phase, and summation over all the phases present is implied (see also chap. 10). X-ray scattering techniques were used to show that porosity present in such fibers was in the form of globular pores of nm size and that the pore fractions ranged from 5 to 25 % (Lipowitz et al. 1990). Channels of nm size diameter form during the early stages of pyrolysis, when rather large volumes of gases are given out. In the later stages of pyrolysis, smaller volumes of gases are given out. In the later stages of pyrolysis, i.e., during densification, these nano-channels suffer a viscous collapse and nanopores are formed. The volume fraction of nanopores decreases with increasing pyrolysis temperature. The reader should note that a higher density and the consequent lower void fraction will result higher elastic modulus and strength of these ceramic fibers.

## 2.10 Comparison of Fibers

A comparison of some important characteristics of reinforcements discussed individually in Sects. 2.2–2.7 is made in Table 2.11, and a plot of strength vs. modulus is shown in Fig. 2.47. We compare and contrast some salient points of these fibers.

First of all, we note that all these high-performance fibers have low density values. If we take the general low density of these fibers as a given, the best of these fibers group together in the top right-hand corner of Fig. 2.47. The reader will also recognize that the elements comprising these fibers pertain to the first two rows of the periodic table. Also to be noted is the fact that, irrespective of whether in compound or elemental form, they are mostly covalently bonded, which is the strongest bond. Generally, such light, strong, and stiff materials are very desirable in most applications, but particularly in aerospace, land transportation, energy-related industry, housing and civil construction, and so on.

Fiber flexibility is associated with the Young’s modulus and the diameter (see Sect. 2.1). In the general area of high-modulus (i.e., high- $E$ ) fibers, the diameter becomes the dominant parameter controlling the flexibility. For a given  $E$ , the smaller the diameter the more flexible it is. Fiber flexibility is a very desirable characteristic if one wants to bend, wind, and weave a fiber in order to make a complex-shaped final product.

Some of these fibers have quite anisotropic characteristics. Consider the situation in regard to thermal properties; in particular, the thermal expansion coefficient of carbon is quite different in the radial and longitudinal directions. This would also be true of any single-crystal fiber or whisker, e.g., alumina single-crystal fiber, which has a hexagonal structure. Polycrystalline fibers such as SiC or  $Al_2O_3$  are isotropic. Carbon, aramid, and polyethylene are anisotropic because the high degree

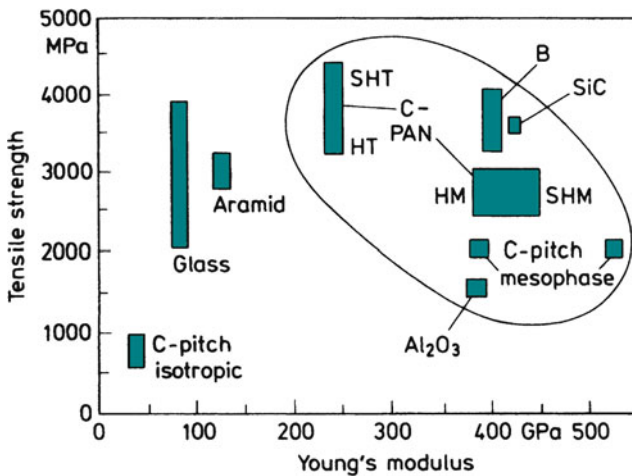


Fig. 2.47 Comparison of different fibers

of alignment, along the axis, of their microstructural units. Ceramic matrix composites can go to very high temperatures, indeed. An important problem that comes up at these very high temperatures ( $>1,500\text{ }^{\circ}\text{C}$ ) is that of fiber (and matrix) oxidation. Carbon fiber, for example, does not have good oxidation resistance at high temperatures. SiC- or  $\text{Si}_3\text{N}_4$ -type ceramic fibers are the only suitable candidates for reinforcement at very high temperatures ( $\sim 1,200\text{--}1,300\text{ }^{\circ}\text{C}$ ) and in air. It would appear that oxide fibers would be the likely candidates, because of their inherent stability in air, for applications at temperatures higher than  $1,300\text{ }^{\circ}\text{C}$  in air. The problem with oxide fibers is their poor creep properties.

Another important characteristic of these high-performance fibers is their rather low values of strain-to-fracture, generally less than 2–3 %. This means that in a CMC, the reinforcement and the matrix may not be much different in terms of strain to fracture. Also, in CMCs the modulus ratio of the reinforcement and the matrix may be 2–3 or as low as 1. This is a very different situation from that encountered in PMCs and MMCs.

**Table 2.11** Properties of reinforcement fibers

Characteristic	PAN-based carbon		Kevlar 49	E glass 8–14	SiC		$\text{Al}_2\text{O}_3$	Boron (W) 100–200
	HM	HS			CVD	Nicalon		
Diameter ( $\mu\text{m}$ )	7–10	7.6–8.6	12	8–14	100–200	10–20	20	100–200
Density ( $\text{g}/\text{cm}^3$ )	1.95	1.75	1.45	2.55	3.3	2.6	3.95	2.6
Young's modulus (GPa)								
Parallel to fiber axis	390	250	125	70	430	180	379	385
Perpendicular to fiber axis	12	20	–	70	–	–	–	–
Tensile strength (GPa)	2.2	2.7	2.8–3.5	1.5–2.5	3.5	2	1.4	3.8
Strain to fracture (%)	0.5	1.0	2.2–2.8	1.8–3.2	–	–	–	–
Coefficient of thermal expansion ( $10^{-6}\text{ K}^{-1}$ )								
Parallel to fiber axis	–0.5–0.1	0.1–0.5	–2–5	4.7	5.7	–	7.5	8.3
Perpendicular to fiber axis	7–12	7–12	59	4.7	–	–	–	–

## References

- Andersson C-H, Warren R (1984) Composites 15:16  
 Bacon R (1973) Chemistry and physics of carbon, vol 9. Marcel Dekker, New York, p 1  
 Baker AA (1983) Metals Forum 6:81  
 Barham PJ, Keller A (1985) J Mater Sci 20:2281  
 Bennett SC, Johnson DJ (1978) Fifth international carbon and graphite conference. Society of the Chemical Industry, London, p 377

- Bennett SC, Johnson DJ (1979) Carbon 17:25
- Bennett SC, Johnson DJ, Johnson W (1983) *J Mater Sci* 18:3337
- Biro DA, Pleizier G, Deslandes Y (1992) *J Mater Sci Lett* 11:698
- Brinker CJ, Scherer G (1990) *The sol-gel science*. Academic, New York
- Brown JR, Chappell PJC, Mathys Z (1992) *J Mater Sci* 27:3167
- Bunsell AR, Piant A (2006) *J Mater Sci* 40:823
- Capaccio G, Gibson AG, Ward IM (1979) *Ultra-high modulus polymers*. Applied Science Publishers, London, p 1
- Chawla KK (1976) *Proceedings of the international conference on the mechanical behavior of materials II*. ASM, Metals Park, OH, p 1920
- Chawla KK (1981) *Mater Sci Eng* 48:137
- Chawla KK (1998a) *Fibrous materials*. Cambridge University Press, Cambridge
- Chawla KK, Bastos AC (1979) *Proceedings of the international conference on the mechanical behavior of materials III*. Pergamon, Oxford, p 191
- de Lamotte E, Perry AJ (1970) *Fibre Sci Technol* 3:157
- DeBolt HE (1982) *Handbook of composites*. Van Nostrand Reinhold, New York, p 171
- DeTeresa SJ, Allen SR, Farris RJ, Porter RS (1984) *J Mater Sci* 19:57
- DiCarlo JA (1985) *J Metals* 37:44
- Diefendorf RJ, Tokarsky E (1975) *Polym Eng Sci* 15:150
- Dobb MG, Johnson DJ, Saville BP (1980) *Philos Trans R Soc Lond A294*:483
- Dresher WH (1969) *J Metals* 21:17
- Ezekiel HN, Spain RG (1967) *J Polym Sci C* 19:271
- Flory PJ (1956) *Proc R Soc Lond* 234A:73
- Fourdeux A, Perret R, Ruland W (1971) *Carbon fibres: their composites and applications*. The Plastics Institute, London, p 57
- Galasso F, Paton A (1966) *Trans Met Soc AIME* 236:1751
- Galasso F, Knebl D, Tice W (1967) *J Appl Phys* 38:414
- Gasson DG, Cockayne B (1970) *J Mater Sci* 5:100
- Haggerty JS (1972) NASA-CR-120948. NASA Lewis Res Center, Cleveland, OH
- Hild DN, Schwartz P (1992a) *J Adhes Sci Technol* 6:879
- Hild DN, Schwartz P (1992b) *J Adhes Sci Technol* 6:897
- Hodd KA, Turley DC (1978) *Chem Br* 14:545
- Hurley GF, Pollack JTA (1972) *Met Trans* 7:397
- Inal OT, Leca N, Keller L (1980) *Phys Status Solidi* 62:681
- Jaffe M, Jones RS (1985) *Handbook of fiber science & technology*, vol 111, High technology fibers. Part A. Marcel Dekker, New York, p 349
- Johnson J, Tyson CN (1969) *Br J Appl Phys* 2:787
- Jones RW (1989) *Fundamental principles of sol-gel technology*. The Institute of Metals, London
- Kalb B, Pennings AJ (1980) *J Mater Sci* 15:2584
- Kaplan SL, Rose PW, Nguyen HX, Chang HW (1988) *SAMPE Quart* 19:55
- Kikuchi T (1982) *Surface* 20:270
- Krukonic V (1977) *Boron and refractory borides*. Springer-Verlag, Berlin, p 517
- Kwolek SL, Morgan PW, Schaeffgen JR, Gultich LW (1977) *Macromolecules* 10:1390
- Kwolek SL, Yang HH (1993) *Manmade fibers: their origin and development*. Elsevier App. Sci, London, p 315
- LaBelle HE (1971) *Mater Res Bull* 6:581
- LaBelle HE, Mlavsky AI (1967) *Nature* 216:574
- Laffon C, Flank AM, Lagarde P, Laridjani M, Hagege R, Olry P, Cotteret J, Dixmier J, Niquel JL, Hommel H, Legrand AP (1989) *J Mater Sci* 24:1503
- Laine RM, Babonneau F (1993) *Chem Mater* 5:260
- Laine RM, Zhang Z-F, Chew KW, Kannisto M, Scotto C (1995) *Ceramic processing science and technology*. Am. Ceram. Soc, Westerville, OH, p 179
- Lee J-G, Cutler IB (1975) *Am Ceram Soc Bull* 54:195

- Li ZF, Netravali AN, Sachse W (1992) *J Mater Sci* 27:4625
- Lipowitz J, Rabe JA, Frevel LK (1990) *J Mater Sci* 25:2118
- Loewenstein KL (1983) *The manufacturing technology of continuous glass fibers*, 2nd edn. Elsevier, New York
- Lowrie RE (1967) In: *Modern composite materials*. Addison-Wesley, Reading, MA, p 270
- Magat EE (1980) *Philos Trans R Soc Lond A296*:463
- Mah T, Hecht NL, McCullum DE, Hoenigman JR, Kim HM, Katz AP, Lipsitt HA (1984) *J Mater Sci* 19:1191
- Milewski JV, Sandstrom JL, Brown WS (1974) *Silicon carbide 1973*. University of South Carolina Press, Columbia, p 634
- Milewski JV, Gac FD, Petrovic JJ, Skaggs SR (1985) *J Mater Sci* 20:1160
- Morgan PW (1979) *Plast Rubber Mater Appl* 4:1
- Murday JS, Dominguez DD, Moran LA, Lee WD, Eaton R (1984) *Synth Met* 9:397
- Northolt MG (1981) *J Mater Sci* 16:2025
- Ozawa S, Nakagawa Y, Matsuda K, Nishihara T, Yunoki H (1978). US patent 4,075,172
- Parkyn B (ed) (1970) *Glass reinforced plastics*. Butterworth, London
- Perret R, Ruland W (1970) *J Appl Crystallogr* 3:525
- Petrovic JJ, Milewski JV, Rohr DL, Gac FD (1985) *J Mater Sci* 20:1167
- Pollack JTA (1972) *J Mater Sci* 7:787
- Riggs JP (1985) *Encyclopedia of polymer science & engineering*, 2nd edn, vol 2. Wiley, New York, p 640
- Sacks MD, Scheiffle GW, Saleem M, Staab GA, Morrone AA, Williams TJ (1995) *Ceramic matrix composites: advanced high-temperature structural materials*. MRS, Pittsburgh, PA, p 3
- Sakka S (1985) *Am Ceram Soc Bull* 64:1463
- Simon G, Bunsell AR (1984) *J Mater Sci* 19:3649
- Singer LS (1979) *Ultra-high modulus polymers*. Applied Science Publishers, Essex, p 251
- Shindo A (1961). *Rep Osaka Ind Res Inst*. No. 317
- Smith P, Lemstra PJ (1976) *Colloid Polym Sci* 15:258
- Smith WD (1977) *Boron and refractory borides*. Springer-Verlag, Berlin, p 541
- Smook J, Pennings AJ (1984) *J Mater Sci* 19:31
- Sowman HG (1988). In *sol-gel technology*. Klein LJ (ed) Noyes Pub., Park Ridge, NJ, p 162
- Talley CP (1959) *J Appl Phys* 30:1114
- Talley CP, Line L, Overman O (1960) *Boron: synthesis, structure, and properties*. Plenum, New York, p 94
- Tanner D, Dhingra AK, Pigliacampi JJ (1986) *J Metals* 38:21
- Toreki W, Batich CD, Sacks MD, Saleem M, Choi GJ, Morrone AA (1994) *Compos Sci Technol* 51:145
- van Maaren AC, Schob O, Westerveld W (1975) *Philips Tech Rev* 35:125
- Vega-Boggio J, Vingsbo O (1978) In: *1978 International conference on composite materials, ICCM/2*. TMS-AIME, New York, p 909
- Warner SB (1995) *Fiber science*. Prentice Hall, Englewood Cliffs, NJ
- Warren R, Andersson C-H (1984) *Composites* 15:101
- Watt W (1970) *Proc R Soc A319*:5
- Watt W, Johnson W (1969) *Appl Polym Symp* 9:215
- Wawner FW (1967) In: *Modern composite materials*. Addison-Wesley, Reading, MA, p 244
- Wax SG (1985) *Am Ceram Soc Bull* 64:1096
- Weintraub E (1911) *J Ind Eng Chem* 3:299
- Wills RR, Mankle RA, Mukherjee SP (1983) *Am Ceram Soc Bull* 62:904
- Wilson DM (1990) In: *Proceedings of the 14th conference on metal matrix, carbon, and ceramic matrix composites*, Cocoa Beach, FL, 17–19 January 1990, NASA Conference Publication 3097, Part 1, p 105
- Wynne KJ, Rice RW (1984) *Annu Rev Mater Sci* 15:297
- Yajima S (1980) *Philos Trans R Soc Lond A294*:419



Yajima S, Okamura K, Hayashi J, Omori M (1976) *J Am Ceram Soc* 59:324  
Zhang Z-F, Scotto S, Laine RM (1994) *Ceram Eng Sci Proc* 15:152

### ***Further Reading***

Bunsell AR (ed) (1988) *Fibre reinforcements for composite materials*. Elsevier, Amsterdam  
Bunsell AR, Berger M (eds) (1999) *Fine ceramic fibers*. Marcel Dekker, New York  
Chawla KK (1998b) *Fibrous materials*. Cambridge University Press, Cambridge  
Donnet J-B, Wang TK, Peng JCM, Rebouillat S (eds) (1998) *Carbon fibers*, vol 3. Marcel Dekker, New York  
Fitzer E (1985) *Carbon fibres and their composites*. Springer-Verlag, Berlin  
Peebles LH (1995) *Carbon fibers*. CRC, Boca Raton, FL  
Watt W, Perov BV (eds) (1985) *Strong fibres*, vol 1 in the handbook of composites series. North-Holland, Amsterdam  
Yang HH (1993) *Kevlar aramid fiber*. Wiley, Chichester

### **Problems**

- 2.1. Nonwoven fibrous mats can be formed through entanglement and/or fibers bonded in the form of webs or yarns by chemical or mechanical means. What are the advantages and disadvantages of such nonwovens over similar woven mats?
- 2.2. Glass fibers are complex mixtures of silicates and borosilicates containing mixed sodium, potassium, calcium, magnesium, and other oxides. Such a glass fiber can be regarded as an inorganic polymeric fiber. Do you think you can provide the chemical structure of such a inorganic fiber chain?
- 2.3. A special kind of glass fiber is used as a medium for the transmission of light signals. Discuss the specific requirements for such an optical fiber.
- 2.4. The compressive strength of aramid fiber is about one-eighth of its tensile stress. Estimate the smallest diameter of a rod on which the aramid fiber can be wound without causing kinks, etc., on its compression side.
- 2.5. Several types of Kevlar aramid fibers are available commercially. Draw schematically the stress–strain curves of Kevlar 49 and Kevlar 29. Describe how much of the strain is elastic (linear or nonlinear). What microstructural processes occur during their deformation?
- 2.6. Aramid fiber, when fractured in tension, shows characteristically longitudinal splitting, i.e., microfibrillation is observed. Explain why.
- 2.7. Describe the structural differences between Kevlar and Nomex (both aramids) that are responsible for their different mechanical characteristics.
- 2.8. What is asbestos fiber and why is it considered to be a health hazard?
- 2.9. Describe the problems involved in mechanical testing of short fibers such as whiskers.